

N 69 21038

**NASA CONTRACTOR
REPORT**

NASA

NASA CR-66665-9

NASA CR-66665-9

**CASE FILE
COPY**

SOFT LANDER PART IX

**Mars Soft Lander Capsule Study (Entry From Orbit)
Analysis of Inflatable Landing Systems**

Prepared by

**MCDONNELL DOUGLAS ASTRONAUTICS COMPANY
EASTERN DIVISION
Saint Louis, Missouri 63166 (314) 232-0232**

for Langley Research Center

NATIONAL AERONAUTICS AND SPACE ADMINISTRATION • WASHINGTON, D.C. • SEPTEMBER 1968

SOFT LANDER PART IX

**Mars Soft Lander Capsule Study (Entry From Orbit)-
Effect of New Environments**

Distribution of this report is provided in the interest of information exchange. Responsibility for the contents resides in the author or organization that prepared it.

Issued by Originator as McDonnell Douglas Astronautics Report G346

Prepared under Contract No. NAS 1-7977 by
MCDONNELL DOUGLAS ASTRONAUTICS COMPANY
EASTERN DIVISION
Saint Louis, Missouri

for Langley Research Center

NATIONAL AERONAUTICS AND SPACE ADMINISTRATION

TABLE OF CONTENTS

	<u>Page</u>
6. Analysis of Inflatable Landing Systems	1
6.1 Summary	2
6.2 Technical Approach	3
6.3 Lander Description	4
6.4 Environments & Design Criteria	7
6.4.1 Environments	7
6.4.2 Design Criteria	7
6.5 Landing System Analysis	9
6.5.1 Test Program	9
6.5.2 Analytical Methods	12
6.5.2.1 Analytical Models	12
6.5.2.2 Parametric Analysis	24
6.6 Lander Parametric Studies	32
6.6.1 Payload Configuration	32
6.6.2 Landing System	38
6.6.2.1 Materials	38
6.6.2.2 Inflation Systems	43
6.6.2.3 Study Results	45
6.7 Additional Design Consideration	53
6.7.1 Payload Attachment	53
6.7.2 Rebound Damping	53
6.7.3 Alternate Landing Systems	54
6.8 Conclusions	56
Appendix A	
Test Results	57

LIST OF PAGES

6. ANALYSIS OF INFLATABLE LANDING SYSTEMS

Use of a high stroke, inflatable landing system for a Mars landing was investigated. This investigation was initiated because of the potential capability of achieving a landing where the equipment experiences much lower landing decelerations than those associated with hard landers and not incurring the cost of terminal propulsion and terminal guidance systems required for soft landers. This study was constrained to landing velocities of 50 to 250 ft/sec and payload weights of 100 to 400 lb. These are considered ranges of interest for a low cost, 1973 Mars lander and are consistent with the use of a parachute as a single, terminal decelerator.

Objectives established for this study were to determine feasibility of an inflatable landing system for Mars landings and to provide preliminary estimates of dynamic characteristics. The key parameter needed to aid in defining feasibility is the energy absorption capability of the torus.

6.1 Summary

A model drop test program was performed to empirically determine attenuation characteristics of the inflatable torus landing system. Test data were used to derive analytical methods required for conducting a parametric analysis. Variation in the following parameters were determined as a function of landing velocity and payload weight:

- o Landing System Weight
- o Maximum Load Factor
- o System Geometry
- o Initial Inflation Pressure

In addition to payload weight, payload shape has an effect on landing system weight. Factors influencing shape, such as payload packaging density and thermal control considerations, were studied also.

The following items needed to define landing system weight were investigated to a depth sufficient for parametric studies:

- o Fabric Materials
- o Elastomers
- o Inflation Systems

Also, payload attachment methods, alternate landing system configurations and methods of rebound damping were investigated and are reported herein.

The primary conclusion reached as a result of this study is that an inflatable torus landing system is feasible for the payload weights, velocities, and study constraints considered. Furthermore, it was verified that a simple analytical model can be used to adequately predict stroke and accelerations for a torus landing flat.

6.2 Technical Approach

The technical approach used to insure achievement of program objectives consists of three parts:

- o Model Tests
- o Analytical Methods
- o Parametric Studies

A rigorous method of analysis for predicting landing loads and energy absorption capability of the torus lander was not available. Therefore, a model test program was conducted to provide information for empirically deriving an analytical method. Because of overall study program objectives and known limitations of the torus model, obtaining highly accurate test data was not required. The main criterion for test data was that it be sufficiently accurate to determine with confidence landing system feasibility. Payload weights, inflation pressures, landing velocities, and landing attitudes (flat and end landings) were the test program variables.

Analytical methods provide the bridge between empirical studies of a model and parametric studies of a Mars lander. It is important that predicted dynamic response of model using selected analytical methods agrees with measured response. After this capability is established, the methods may be used with confidence to study full scale, Mars landers.

The last part of the approach involves conducting parametric studies consisting primarily of defining design requirements for torus landing system. Results from these parametric studies provide capability for rapidly selecting torus geometrical proportions and inflation pressures required to achieve a minimum landing system weight for a lander designed to particular velocities. In addition, trade-offs can be made easily between weight and landing accelerations.

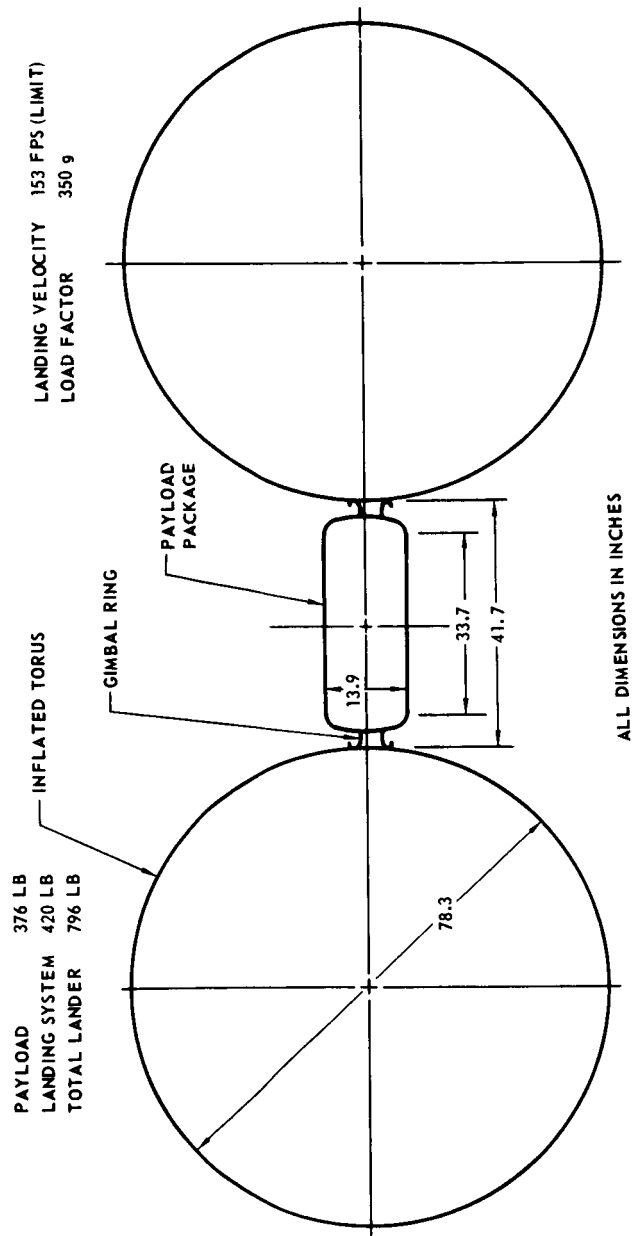
6.3 Lander Description

For this study, the lander is assumed to be comprised of two parts: landing system and payload. The landing system consists of inflatable torus and inflation system. The payload consists of science equipment, payload structure, gimbal ring, and insulation. A typical lander design is shown in Figure 6.3-1.

A typical landing operation includes the following events. A supersonic ring sail parachute is deployed at an altitude of 10,000 feet and the lander is released from the aeroshell by explosive bolts immediately thereafter. Separation from the aeroshell is by differential drag. As the lander descends, the torus is inflated. Approximately 40-50 seconds are allowed for torus inflation. Shorter inflation times may be preferred in a dense atmosphere where the increased drag would lengthen descent time, thus cutting post landed view time. At an altitude of 100 feet the parachute is released, along with the inflation system pressure tank, by firing explosive bolts and the lander free-falls to the surface. Vertical velocity at the time of parachute release is about 120 ft/sec and increases to 130 ft/sec at surface contact. To determine limit velocity for landing system design, it is assumed that the lander has achieved a horizontal velocity equivalent to nominal wind velocity of 118 ft/sec and landing occurs on a 20 degree slope. Based on these assumptions, the limit velocity (component normal to 20 degree slope) is 153 ft/sec. After the lander comes to rest, the payload package rotates to achieve an upright position (180° rotation if required) and begins to deploy the equipment. Lander operation duration is 3 day minimum with a design objective of 90 days.

The typical design, shown in Figure 6.3-1, is a single, non-venting inflatable torus with a flat cylindrical payload installation. The total lander weight is 796 pounds, with 420 pounds of the total attributed to landing system including torus and inflation system. When inflated to the nominal design pressure of 10 psig, the torus has an outside diameter of 198.3 inches, an inside diameter of 41.7 inches, and a cross-sectional radius of 78.3 inches.

TYPICAL TORUS GEOMETRY



The inflatable torus is constructed from Nomex fabric coated with a silicone elastomer for gas retention. An increase in fabric strength is required in the area around the payload gimbal ring to accommodate higher loads which exist in that area.

The payload package is supported by a single gimbal ring which provides a single axis pivot for payload rotation. Thermal control of equipment is provided by insulation and isotope heaters. The payload contains 39 pounds of science equipment including, facsimile camera, gas chromatograph, mass spectrometer, soil sampler, life detector, atmospheric hygrometer, soil hygrometer and probe, atmosphere temperature sensor, atmosphere pressure sensor, and anemometer.

6.4 Environments and Design Criteria

6.4.1 ENVIRONMENTS - The landing system is exposed to many environments during the various mission phases. In addition, materials and components are qualified using environments significantly more severe than those expected in flight. Those environments having significant effects on design of an inflatable structure are the heat sterilization environment for qualifying parts and materials, vacuum environment during interplanetary cruise, and Mars atmospheric environment during the post-landing phase.

Heat Sterilization - Heat sterilization environment for qualification of parts and materials is as follows: six cycles of 96 hours each at 275°F. Total time at temperature is 576 hours. Atmosphere is dry nitrogen.

Vacuum - The landing system is exposed to the vacuum of space for 230 days at temperatures ranging from -100°F to +100°F.

Mars Atmosphere - After the lander comes to rest on the surface of Mars, it is exposed to the following environments: atmospheric pressure, 4.0 mb to 20 mb; temperature, -154°F to +120°F; winds, 0 to 220 ft/sec (118 ft/sec nominal).

6.4.2 DESIGN CRITERIA - Specific criteria related to initial lander conditions, factors of safety, and pressurization factors are defined. These criteria provide a basis for defining design conditions and resulting structural requirements of the landing system.

Initial Conditions

Velocity, 50 to 250 ft/sec (limit)

Payload Weight, 100 to 400 lb

Factors of Safety

Landing System - Designed for ultimate total energy [(limit kinetic plus limit potential energy) x 1.25].

Payload Structure - Designed for ultimate loads (limit loads resulting from limit total energy x 1.25).

Pressurization Factors

Pressure Vessels - Designed to withstand proof pressure of 1.67 times maximum operating pressure without yielding. Designed to withstand burst pressure of 2.22 times maximum operating pressure without failure.

Inflatable Structure - Designed for ultimate loads (limit loads resulting from limit total energy x 2.5).

The landing system shall be designed to land on surfaces containing slopes from 0 to 20 degrees with bearing capacities ranging from 200 lb/ft² to infinity. Landing system shall maintain sufficient pressure for three days to support payload above the surface.

6.5 Landing System Analysis

Static and dynamic tests of an inflatable torus lander model were conducted in order to obtain empirical data needed to design the landing system. Based on these test data, analytical methods were derived to be used for parametric studies. In this section, the test program is briefly discussed and analytical methods are presented. Further discussion of test program is given in the Appendix.

6.5.1 TEST PROGRAM - Key parameters to be determined for design of inflatable landing systems are stroke and acceleration. Model tests were conducted to determine values of these parameters during flat and end landings for various landing velocities, inflation pressures, and payload weights.

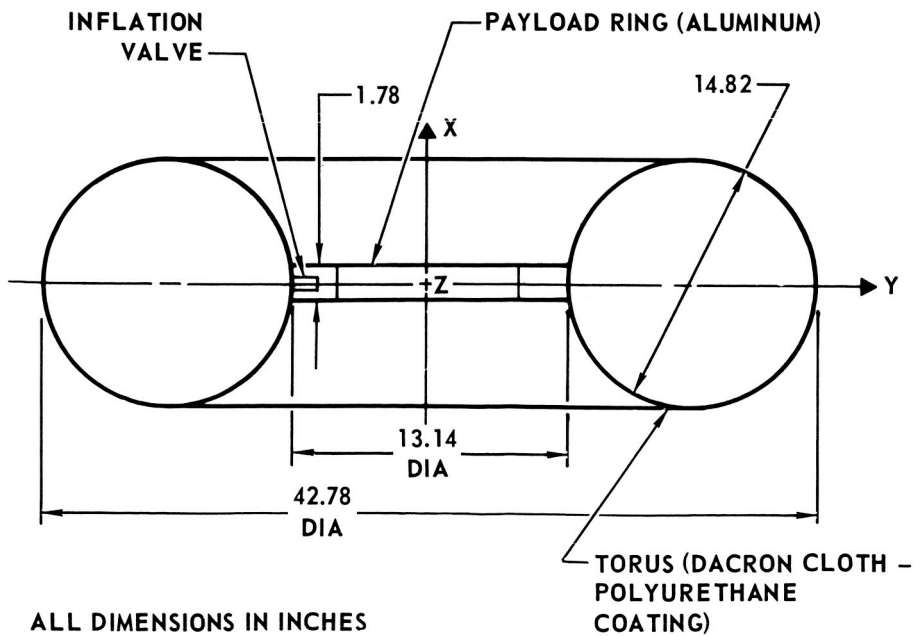
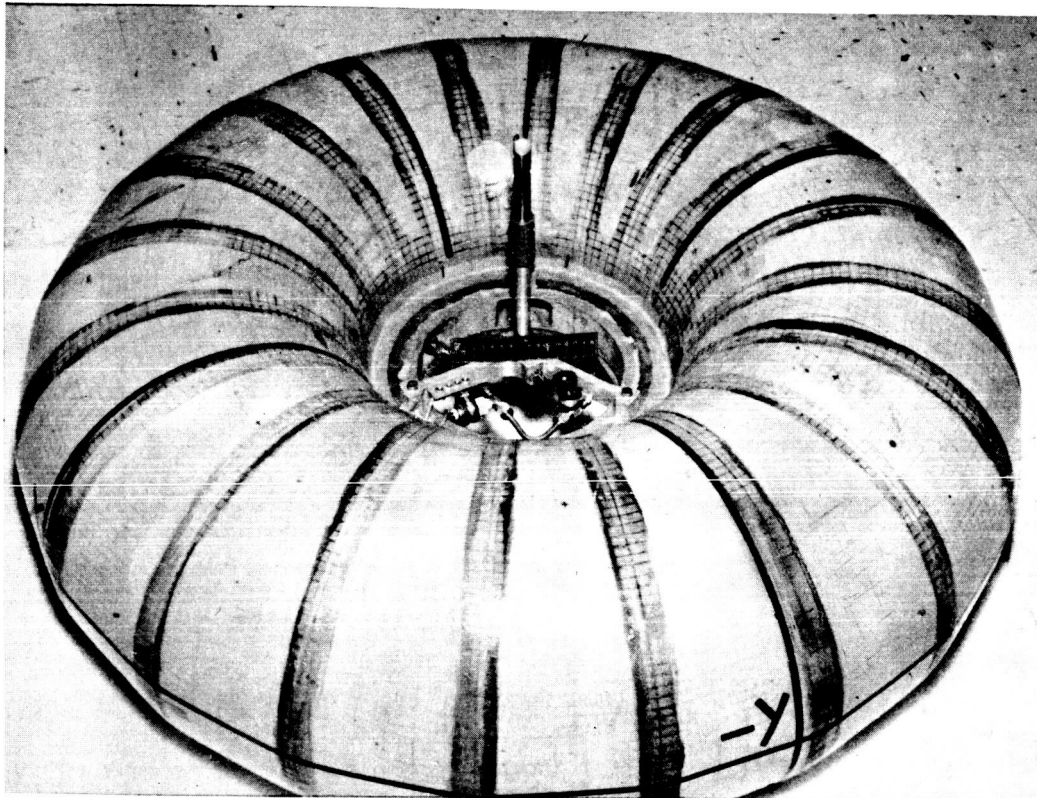
Model Description - The test model, shown in Figure 6.5.1-1, consists of an inflated torus continuously attached to an inner payload ring. The torus was constructed of Dacron fabric coated with polyurethane sealant. Grid lines were painted on the external surface of the torus to aid in defining lander orientation at impact and observing torus deformations during the attenuation process. Different payload weights were obtained by attaching steel plates to the aluminum alloy payload ring. Provisions for mounting test instrumentation were also incorporated in the payload ring design. An inflation valve is accessible through the payload ring.

Static Tests - Static tests were conducted to determine payload stroke and internal torus pressure as a function of load applied to payload ring. Tests were conducted for both flat and end loading orientations as shown in Figure 6.5.1-2. Load-stroke relationships obtained from these tests are used in conjunction with analytical models discussed later.

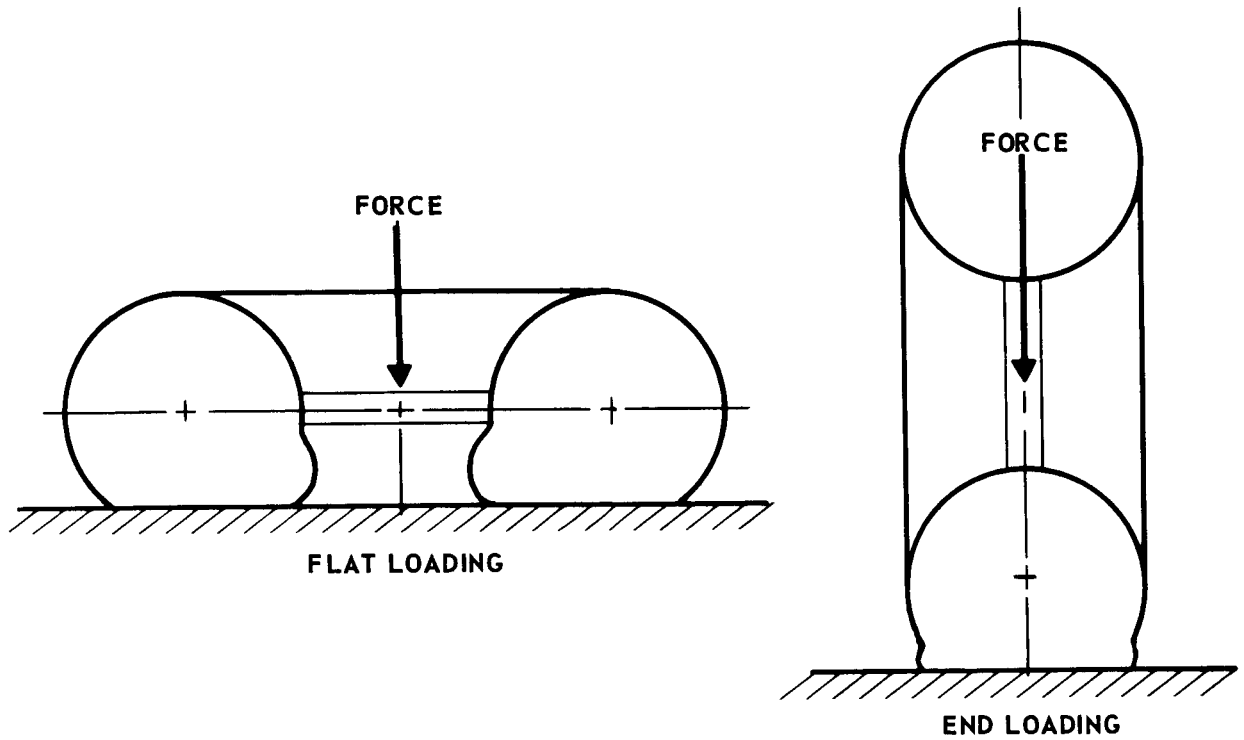
Three flat loading tests were performed with initial torus pressures of 2.0, 4.0, and 6.0 psig. End loading tests were conducted at 2.0 and 4.0 psig. For each test, load was applied until the desired maximum stroke was obtained.

Dynamic Tests - Drop tests were conducted to determine the effects of landing velocity, payload weight and torus pressure on payload stroke and acceleration. Tests were conducted in the Zero Gravity Research Facility at

TEST MODEL DESCRIPTION



MODEL STATIC TEST POSITIONS



the NASA Lewis Research Center in Cleveland, Ohio. Chamber pressure was about 5 mb for all tests in order to simulate Mars atmospheric pressure. Seventeen flat and seven end drop tests were performed with payload weight ranging from 4.1 pounds to 11.0 pounds and inflation pressures ranging from 2.1 psig to 6.0 psig. Landing velocities varied from 7 ft/sec to 100 ft/sec.

For a given payload weight, inflation pressure, and landing velocity; the maximum payload stroke resulting from end landing was approximately twice that obtained from flat landings. However, accelerations experienced by the payload during end landings were about one-half those experienced during flat landings.

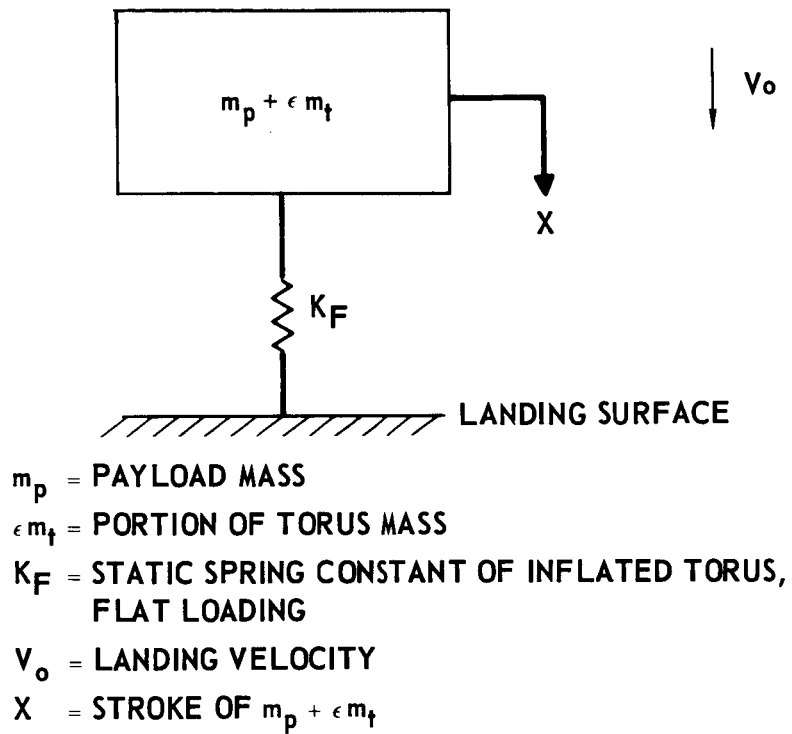
6.5.2 ANALYTICAL METHODS - In the following paragraphs, analytical methods used for parametric studies of inflatable torus landing systems are presented. Analytical models used to predict payload stroke and acceleration are described. Verification of selected models is shown by comparing predicted values with test data. In addition, pertinent steps required in parametric analyses are presented.

6.5.2.1 Analytical models. - For parametric studies, an idealized analytical model is required to represent the landing system during impact. A number of analytical models were studied to select a model for predicting both stroke and acceleration. Although the actual landing system is composed of many degrees of freedom, a simple dynamic model consisting of a minimum number of degrees of freedom is adequate provided it closely approximates behavior of the actual lander.

The simplest dynamic model for flat landing is the single degree of freedom system shown in Figure 6.5.2-1. Mass is composed of the payload mass (m_p) and a portion of the torus mass (ϵm_t). The spring (K_F) is the static spring constant of torus determined for flat loading. For a given payload mass, torus mass, and spring constant; dynamic behavior of the system is altered by changing ϵ . The equation of motion for this system is:

$$(m_p + \epsilon m_t) \ddot{X} + K_F X = (m_p + \epsilon m_t) g \quad (1)$$

PRELIMINARY ANALYTICAL MODEL
FOR FLAT LANDING



Initial conditions are assumed to be:

$$X(0) = 0$$

$$\dot{X}(0) = v_0$$

When the gravitational force term in Equation (1) is neglected, payload response is expressed as:

$$X = \frac{V_0}{\omega_n} \sin(\omega_n t)$$

$$\text{Where, } \omega_n = \sqrt{\frac{K_F}{(m_p + \epsilon m_t)}}$$

Determining adequacy of this model for predicting response of torus is accomplished in the following manner.

Results of static tests, discussed in Appendix A, were used to determine the spring constant (K_F). Since the actual spring rate is slightly non-linear and a linear spring is used in analytical model, an effective linear spring is derived from test results. The effective spring constant is determined by equating the energy stored in the linear spring when subjected to a given stroke to the area under the static load-stroke curve up to the same stroke of interest.

Measured stroke and acceleration time histories for a typical dynamic test are shown as dashed curves in Figure 6.5.2-2. Predicted response using the single mass model is represented by the solid curves. Good agreement between predicted and actual stroke is obtained for $\epsilon = 0.66$. However, for $\epsilon = 0.66$, predicted acceleration is considerably lower than measured acceleration. By selecting a different value of ϵ , accelerations could be matched but the model would predict incorrect strokes.

The two degree of freedom model, shown in Figure 6.5.2-3, was finally selected for predicting response of the torus during flat landing. Equations

COMPARISON OF MEASURED WITH PREDICTED STROKE AND AND ACCELERATION FOR TYPICAL FLAT LANDING

- MEASURED RESPONSE
- PREDICTED RESPONSE USING PRELIMINARY
MODEL, $\epsilon = 0.66$
- IMPACT VELOCITY = 32 FT/SEC
- INFLATION PRESSURE = 2.1 PSIG
- PAYLOAD WEIGHT = 4.1 LB
- TORUS WEIGHT = 4.6 LB

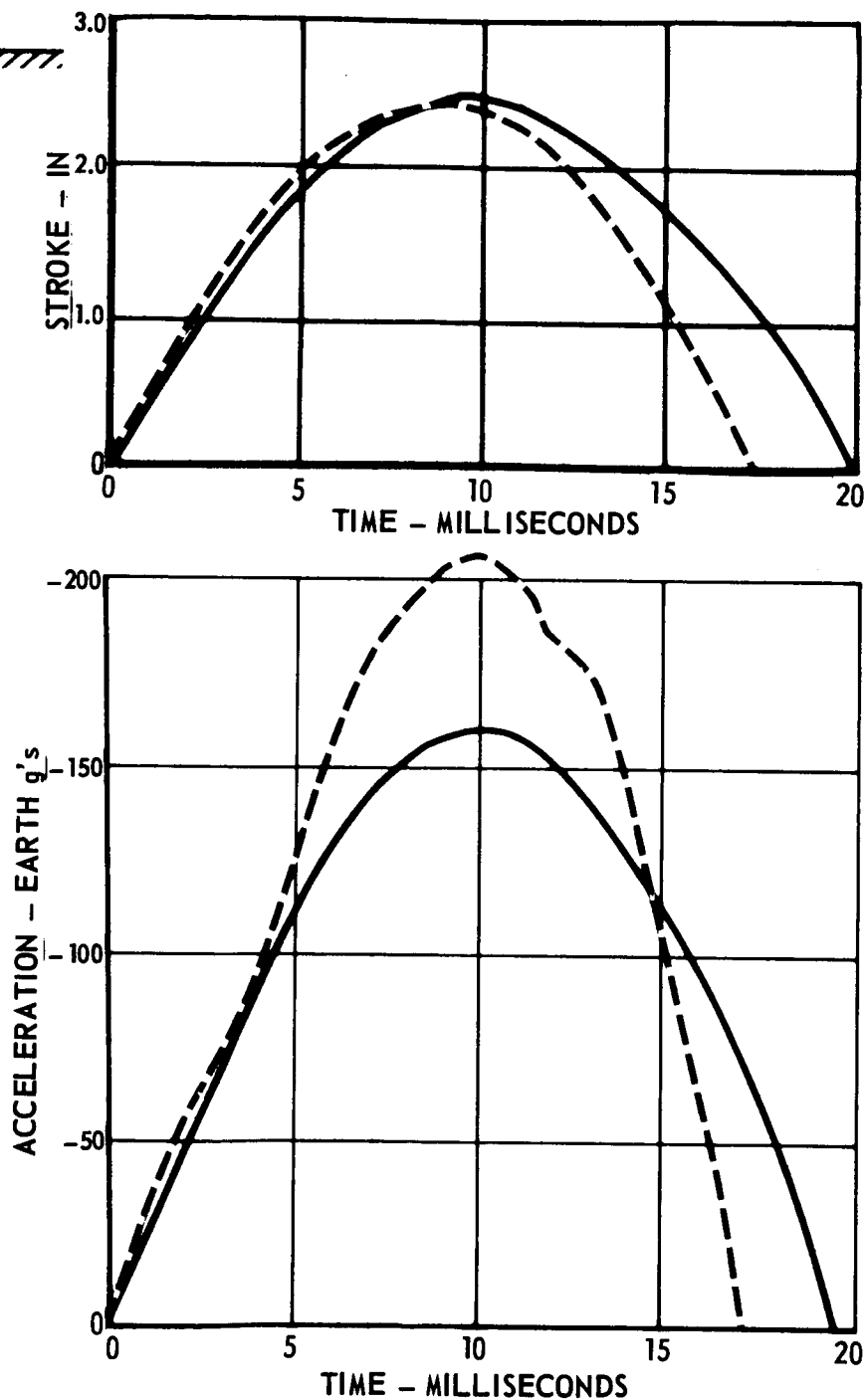
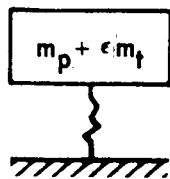
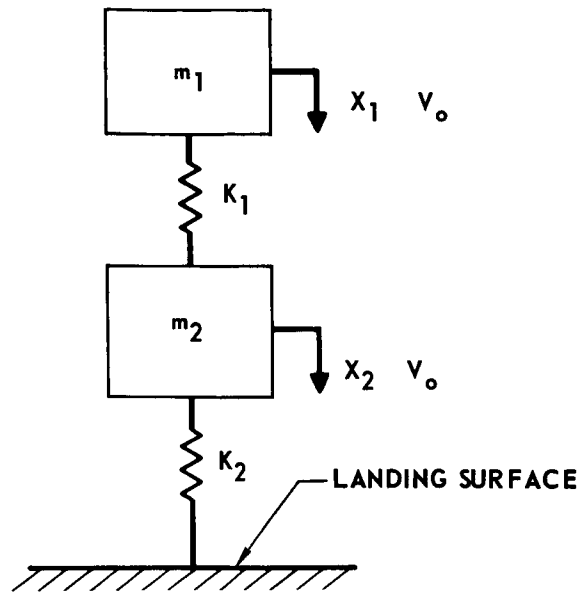


FIGURE 6.5.2-2

SELECTED ANALYTICAL MODEL FOR FLAT LANDING



m_1 = PAYLOAD MASS, m_p
 m_2 = PORTION OF TORUS MASS, ϵm_t
 K_1 = SPRING CONSTANT OF m_1
 K_2 = SPRING CONSTANT OF m_2
 v_0 = LANDING VELOCITY
 x_1, x_2 = STROKE OF m_1 AND m_2 RESPECTIVELY

NOTE:

$$\frac{1}{K_1} + \frac{1}{K_2} = \frac{1}{K_F}$$

WHERE K_F = STATIC SPRING CONSTANT OF INFLATED TORUS, FLAT LOADING

LETTING $\alpha = \frac{K_1}{K_F}$

THEN $K_2 = \left(\frac{-\alpha}{\alpha - 1} \right) K_F$

of motion for this system are;

$$m_1 \ddot{X}_1 + K_1 X_1 - K_1 X_2 = m_1 g \quad (2)$$

$$m_2 \ddot{X}_2 + (K_1 + K_2) X_2 - K_1 X_1 = m_2 g \quad (3)$$

with the initial conditions

$$X_1(0) = X_2(0) = 0$$

$$\dot{X}_1(0) = \dot{X}_2(0) = V_0$$

where V_0 is the impacting velocity of the landing system.

It is assumed that X_1 is equal to payload stroke, m_1 is equal to the payload mass (m_p), m_2 is some portion of the torus mass (m_t), and the combination of springs K_1 and K_2 in series duplicates the static spring constant of the inflated torus (K_F).

These assumptions are expressed as follows:

$$m_1 = m_p$$

$$m_2 = \epsilon m_t$$

$$K_1 = \alpha K_F$$

$$K_2 = \left(\frac{\alpha}{\alpha - 1} \right) K_F$$

where

ϵ = that portion of torus mass included in dynamic model

α = that portion of torus static spring rate (K_F) included in K_1

Neglecting the gravitational force terms in Equation (2) and (3), response of the payload is expressed as:

$$X_1 = \left[\frac{-(\omega_2)^2}{(\omega_1)^2 - (\omega_2)^2} \right] \frac{V_0}{\omega_1} \sin \omega_1 t + \left[\frac{(\omega_1)^2}{(\omega_1)^2 - (\omega_2)^2} \right] \frac{V_0}{\omega_2} \sin \omega_2 t$$

In the above expression, frequencies ω_1 and ω_2 are roots of the following polynomial:

$$(\omega_n)^4 - \left[\frac{\alpha}{m_p} + \frac{(\alpha)^2}{\varepsilon(\alpha - 1) m_t} \right] K_F (\omega_n)^2 + \frac{(\alpha)^2 (K_F)^2}{\varepsilon(\alpha - 1) m_p m_t} = 0$$

for $n = 1$ and 2 .

From test results the following values for α and ε were determined which duplicate torus response.

$$\alpha = 8.0$$

$$\varepsilon = 0.6$$

Predicted stroke and acceleration using the two degree of freedom model is compared with measured response for a typical dynamic test in Figure 6.5.2-4. Good agreement exists for both stroke and acceleration. In addition, comparisons of predicted maximum stroke and maximum acceleration with test results are shown in Figure 6.5.2-5 through 6.5.2-7. As can be seen from these figures, good agreement is obtained between predicted response of the torus and test results for different payload weights, inflation pressures, and landing velocities.

For end landing, a single degree of freedom model is used to predict response of the torus. This model, shown in Figure 6.5.2-8, consists of a mass equal to the sum of payload and torus masses, and a single linear spring. The spring rate is obtained from static tests.

The equation of motion for this system is:

$$(m_p + m_t) \ddot{Y} + K_E Y = (m_p + m_t) g \quad (4)$$

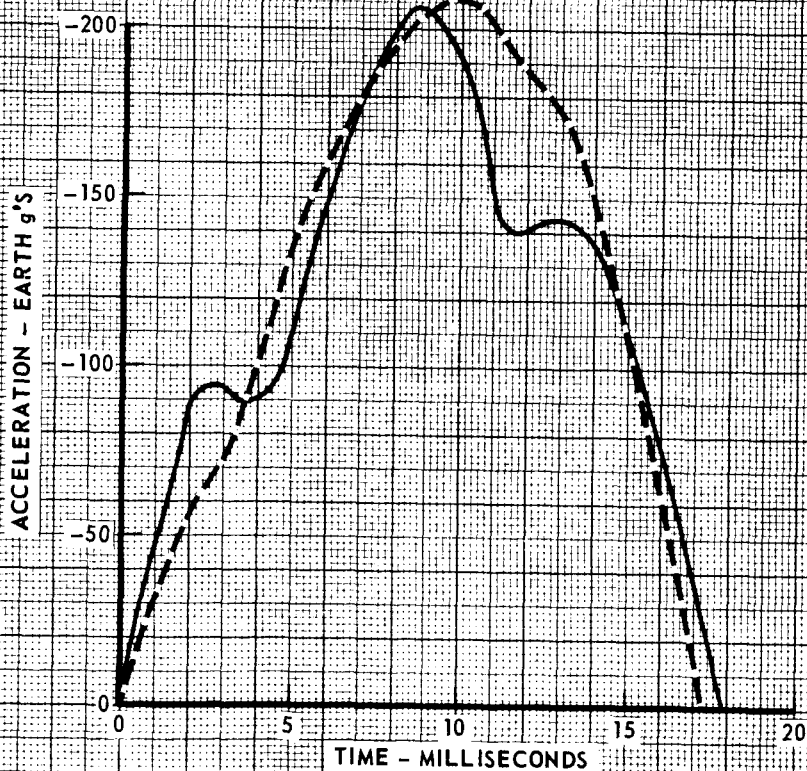
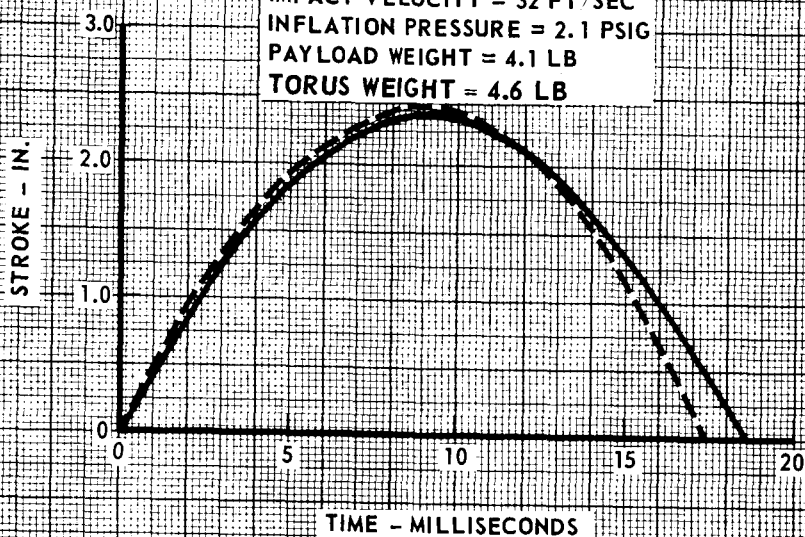
Initial conditions are assumed to be:

$$Y(0) = 0$$

$$\dot{Y}(0) = V_0 \text{ (impact velocity)}$$

COMPARISON OF MEASURED WITH PREDICTED STROKE AND ACCELERATION FOR TYPICAL FLAT LANDING CONDITION

- - - - - MEASURED RESPONSE
 ———— PREDICTED RESPONSE USING
 SELECTED ANALYTICAL
 MODEL, $\epsilon = 0.6$, $\alpha = 8.0$
 IMPACT VELOCITY = 32 FT/SEC
 INFLATION PRESSURE = 2.1 PSIG
 PAYLOAD WEIGHT = 4.1 LB
 TORUS WEIGHT = 4.6 LB



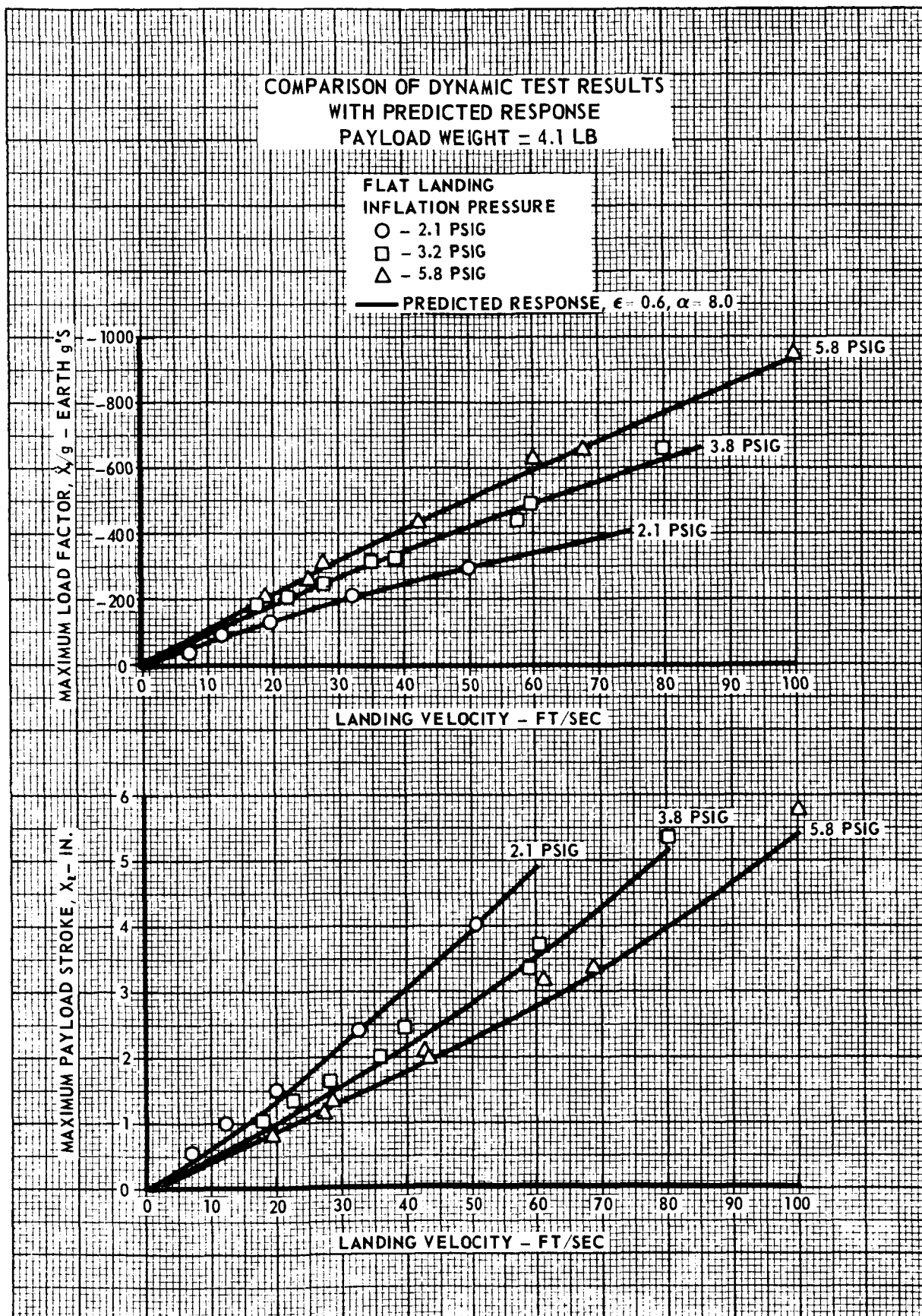


FIGURE 6.5.2-5

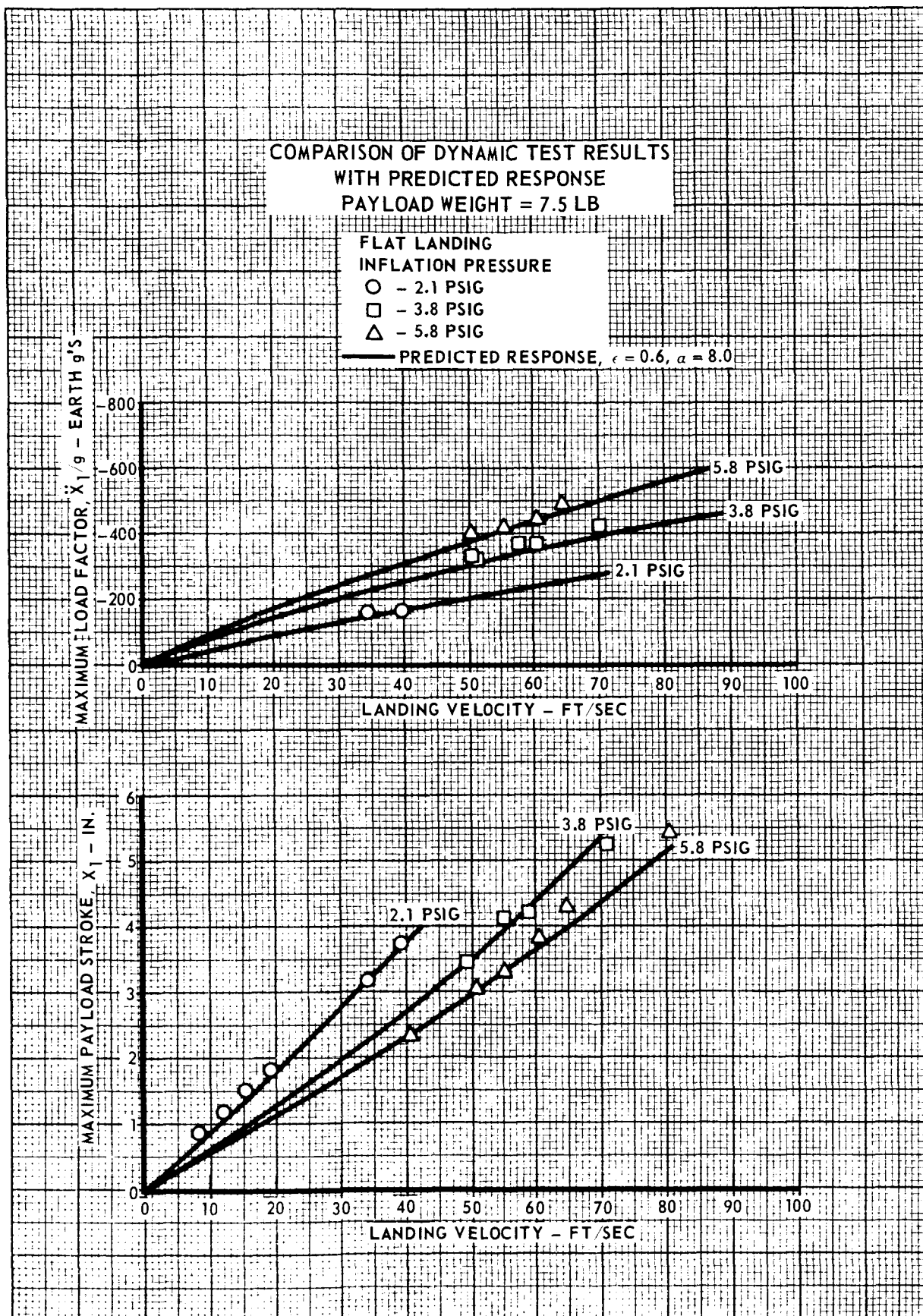


FIGURE 6.5.2-6

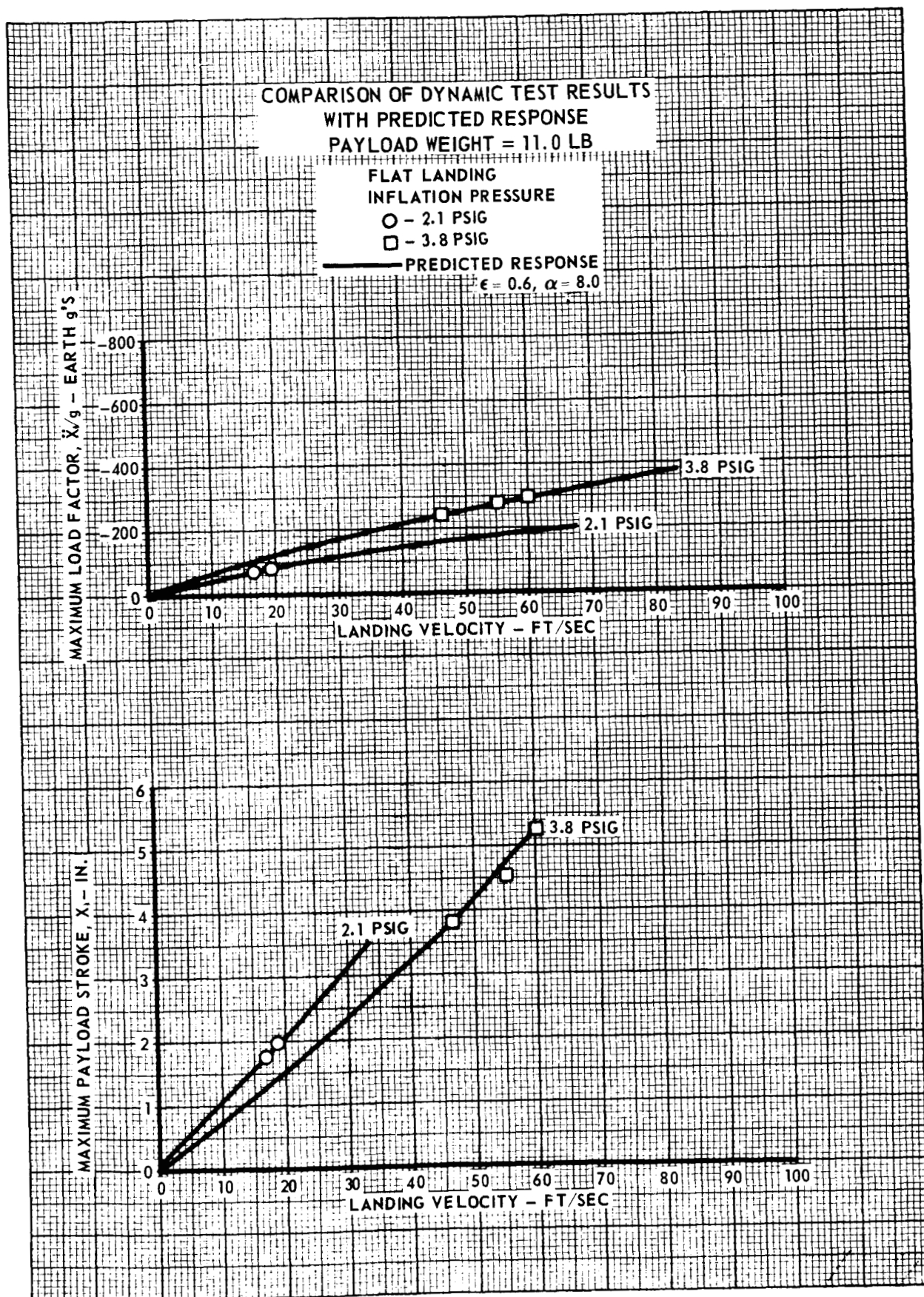
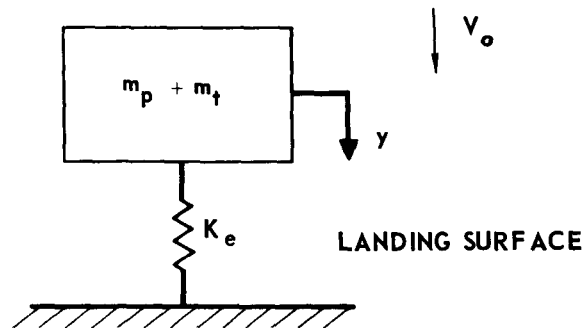


FIGURE 6.5.2-7

6.5-14

ANALYTICAL MODEL FOR END LANDING



m_p = PAYLOAD MASS

m_t = TORUS MASS

K_e = STATIC SPRING CONSTANT OF INFLATED TORUS, END LOADING

V_o = LANDING VELOCITY

y = STROKE OF $m_p + m_t$

Neglecting the gravitational force term in Equation (4), payload response is expressed as:

$$Y = \frac{V_0}{\omega_n} \sin (\omega_n t)$$

where

$$\omega_n = \sqrt{\frac{K_E}{(m_p + m_t)}}$$

Comparisons of test results with predicted response using this model are shown in Figures 6.5.2-9 and 6.5.2-10. Agreement between predicted and measured response for end landings is not as good as it is for flat landings. However, the basic purpose of end landing tests was to verify that sufficient stroke capability existed and that accelerations were much lower than for flat landings. The selected model was sufficient to fulfill these objectives.

6.5.2.2 Parametric analysis. - In order to facilitate computations required for conducting parametric studies, a computer program was written. This program computes landing system weight, maximum load factor and landing velocity as a function of payload size and weight, inflation pressure, and torus size.

Steps used in the parametric analysis are listed below.

1. Select payload weight and size.
2. Assume lander radius.
3. Assume inflation pressure.
4. Compute torus and inflation system weights.
5. Compute allowable landing velocity and associated payload acceleration.
6. Repeat Steps 2 through 5 until the desired landing velocity and acceleration are achieved.

In Step (4) maximum torus internal loads are assumed to result from flat landing and occur at the intersection of the payload ring and torus. These loads are determined in the following manner. Torus deformations resulting from flat static loading are shown in Figure 6.5.2-11. If similar deformations are assumed to occur during dynamic loading, it is possible to determine

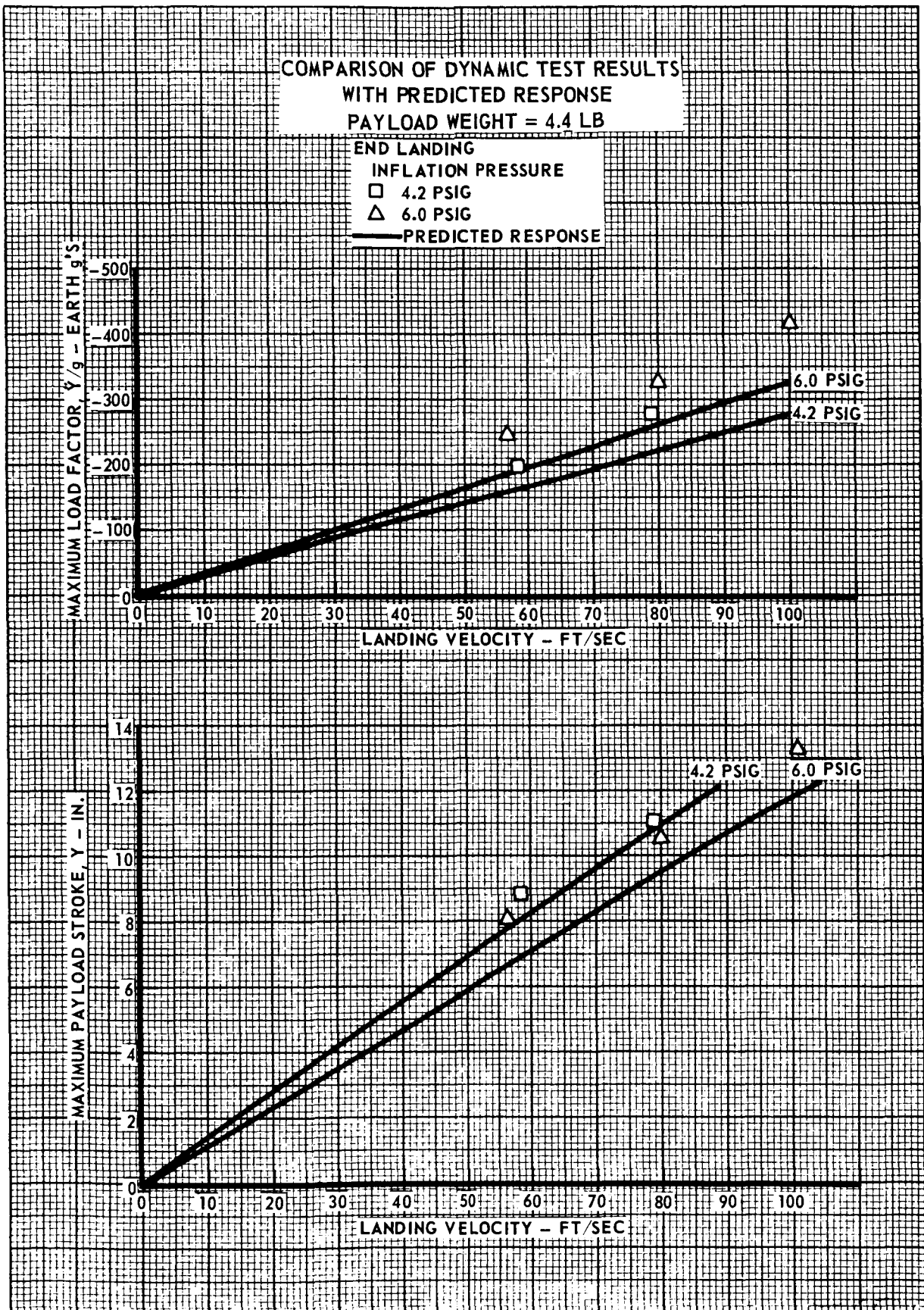


FIGURE 6.5.2-9

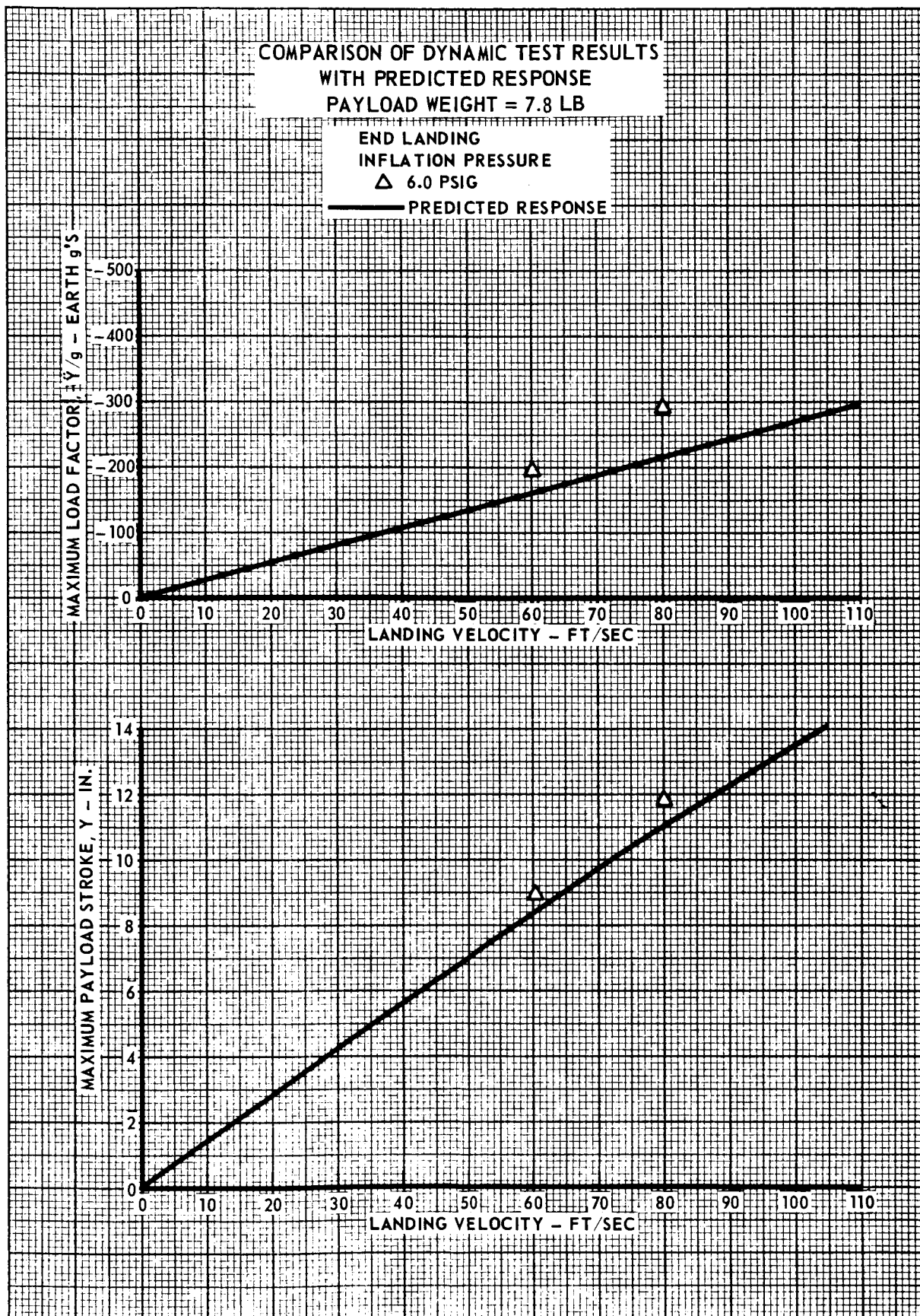
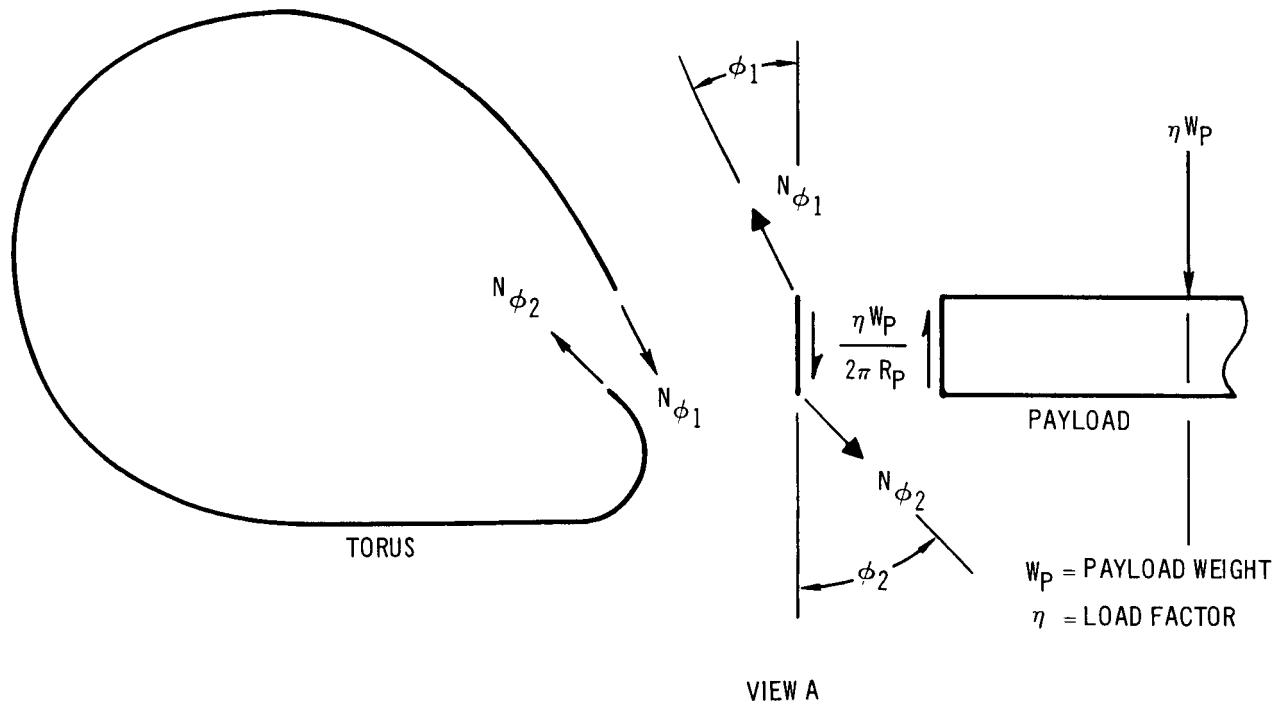
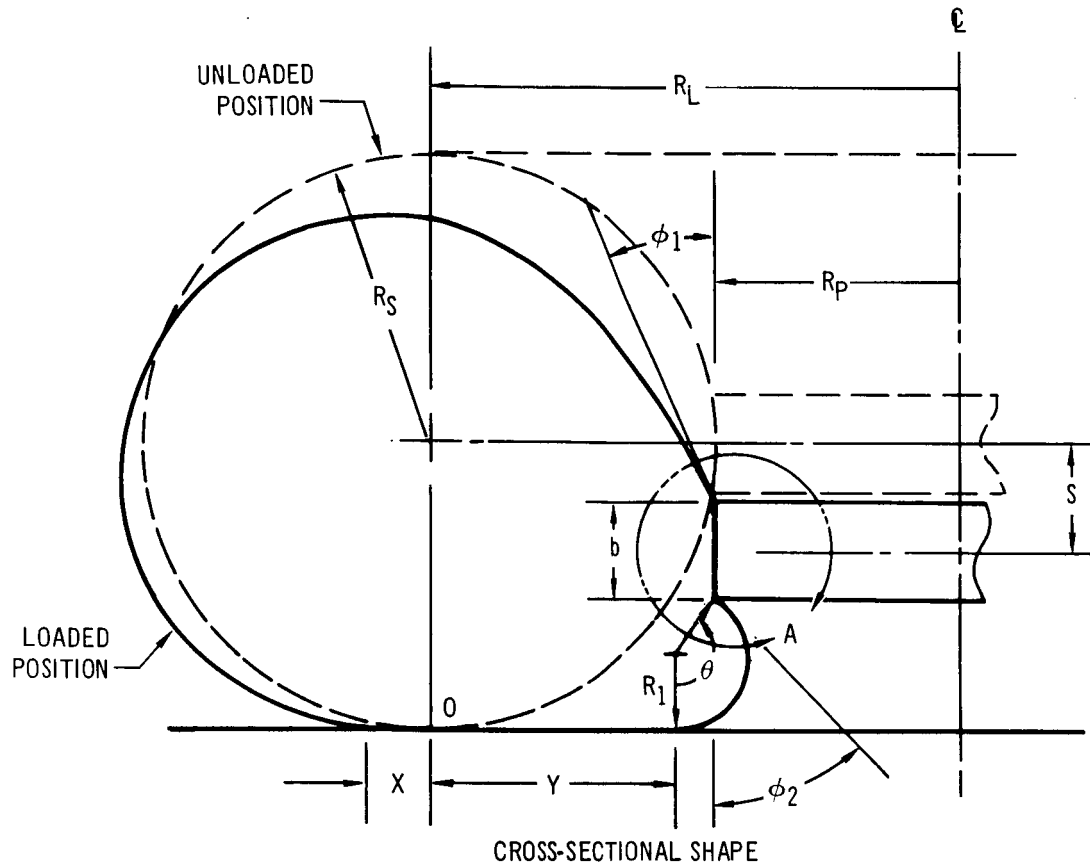


FIGURE 6.5.2-10

TORUS DEFORMATIONS DURING FLAT STATIC LOADING



internal loads at the intersection of torus and payload ring as shown in View A of Figure 6.5.2-11. Maximum meridional load in the torus (N_{ϕ_1}) is defined by the following expression:

$$N_{\phi_1} = \frac{\eta W_p}{2\pi R_p \cos \phi_1} + \frac{PR_1 \cos \phi_2}{\cos \phi_1} \quad (5)$$

where: η = maximum load factor on payload
 W_p = weight of payload
 P = internal pressure of deformed torus
 R_p = payload radius
 R_1 = local radius of curvature of deformed torus (Reference Figure 6.5.2-11)
 ϕ_1, ϕ_2 = angles of deformation (Reference Figure 6.5.2-11)

During static tests, angle ϕ_1 and footprint dimension X were measured in addition to load, pressure and stroke. Variation of angle ϕ_1 , dimension X and volume ratio (V_i/V_d) with stroke and torus cross-sectional radius (R_s) are represented by the following equations:

$$\phi_1 = 0.422 (S/R_s) \quad (6)$$

$$X = 0.005 R_s + 0.690S - 0.525 S^2/R_s \quad (7)$$

$$V_i/V_d = 0.998 + 0.049 \left(\frac{S}{R_s}\right) + 0.240 \left(\frac{S}{R_s}\right)^2 \quad (8)$$

where: V_i = initial undeformed torus volume
 V_d = volume of deformed torus

With the above parameters known, internal pressure (P) can be defined, and dimension y can be analytically determined by assuming that point "0" (Figure 6.5.2-11) does not move radially during the stroking process. The equations for y and pressure are,

$$Y = 0.005 R_s + 2.409S - 1.171 \frac{S^2}{R_s} \quad (9)$$

$$P = (P_i + P_\infty) \left(\frac{V_i}{V_d}\right) - P_\infty \quad (10)$$

where: P_i = initial inflation pressure
 P_∞ = ambient pressure

Angle ϕ_2 and radius R_1 can now be defined in terms of torus radius (R_s) and payload depth (b).

$$\phi_2 = \theta - \frac{\pi}{2} \quad (11)$$

$$\text{and} \quad R_1 = \frac{\pi R_s - 2Y - b}{2\theta} \quad (12)$$

$$\text{where} \quad \frac{\sin \theta}{2\theta} = \frac{R_s - Y}{\pi R_s - 2Y - b} \quad (13)$$

Although torus thickness at the intersection of the payload and torus is based on Equation (5), thickness is reduced in proportion to internal meridional loads in three steps as shown in Figure 6.5.2-12. Depending on geometrical proportions, considerable difference in weight can exist between a minimum weight torus and a single thickness torus. A minimum weight torus is one having fabric strength tailored to meridional loads. Relative thicknesses of a minimum weight torus, single thickness torus, and stepped thickness torus are shown in Figure 6.5.2-12. By changing fabric thickness in three steps, it is possible to achieve up to 85 percent of the potential weight saving associated with a minimum weight design.

As discussed in Section 6.6.2.2, a stored pressurized gas system is used to inflate the torus. Weight of the pressure tank accounts for majority of inflation system weight. The following weight equation, used in parametric analyses, applied to spherical pressurization tanks.

$$W_{\text{TANK}} = \frac{2\pi r^3 \rho p (\text{FS})}{F_{\text{TU}}} \quad (14)$$

where,

r = tank radius
 ρ = material density
 p = storage pressure

COMPARISON OF ACTUAL AND REQUIRED CLOTH THICKNESSES FOR TYPICAL TORUS GEOMETRY

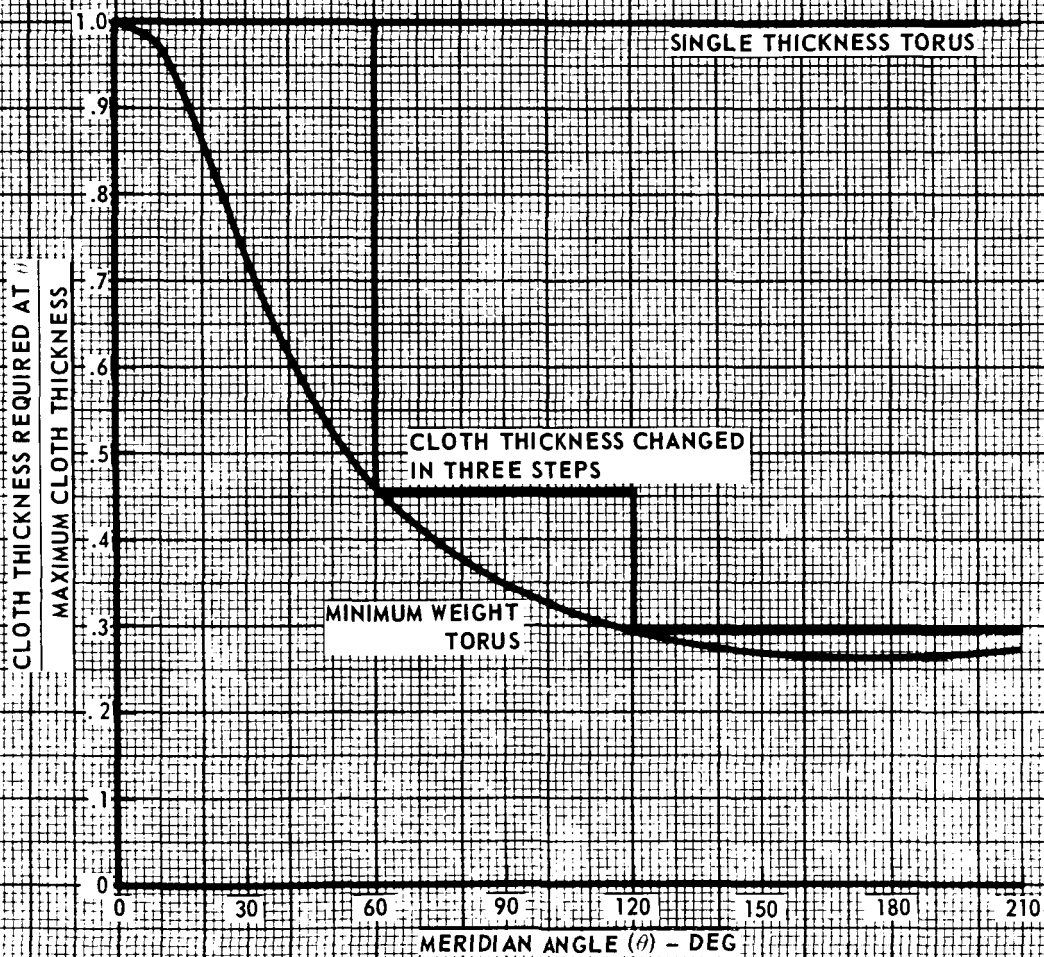
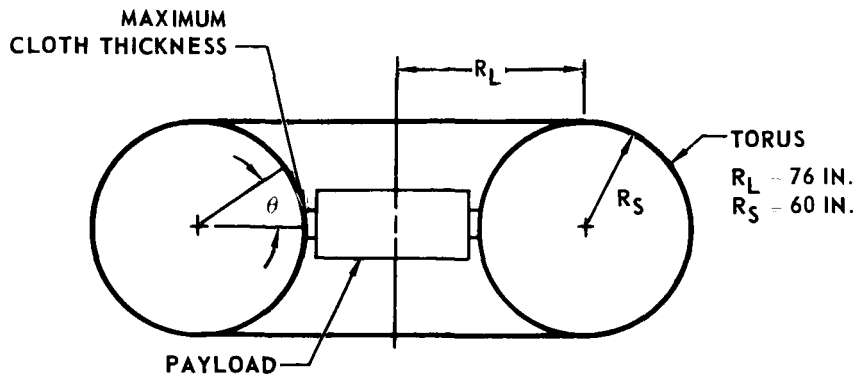


FIGURE 6.5.2-11

FS = factor of safety

F_{TU} = ultimate tensile strength of tank material

Volume of storage tank required (V) is related to torus volume and pressure by the following expression:

$$V = \frac{p_i V_i}{p} \quad (15)$$

For parametric studies a 5 000 psi storage pressure was assumed. Volume of a spherical tank is defined by the following expression:

$$V = \frac{4}{3} \pi r^3 \quad (16)$$

Combining equations (15) and (16),

$$r = \sqrt[3]{\frac{3p_i V_i}{4\pi p}} \quad (17)$$

Tank radius (r) defined by Equation (17) was used to determine tank weight in Equation (14).

The two mass model discussed earlier, with $\alpha = 8.0$ and $\epsilon = 0.6$, is used in Step (5) to determine maximum load factor and landing velocity.

Footprint area for flat landing is defined by the following equation:

$$A = \pi[2R_L(X + Y) + X^2 - Y^2] \quad (18)$$

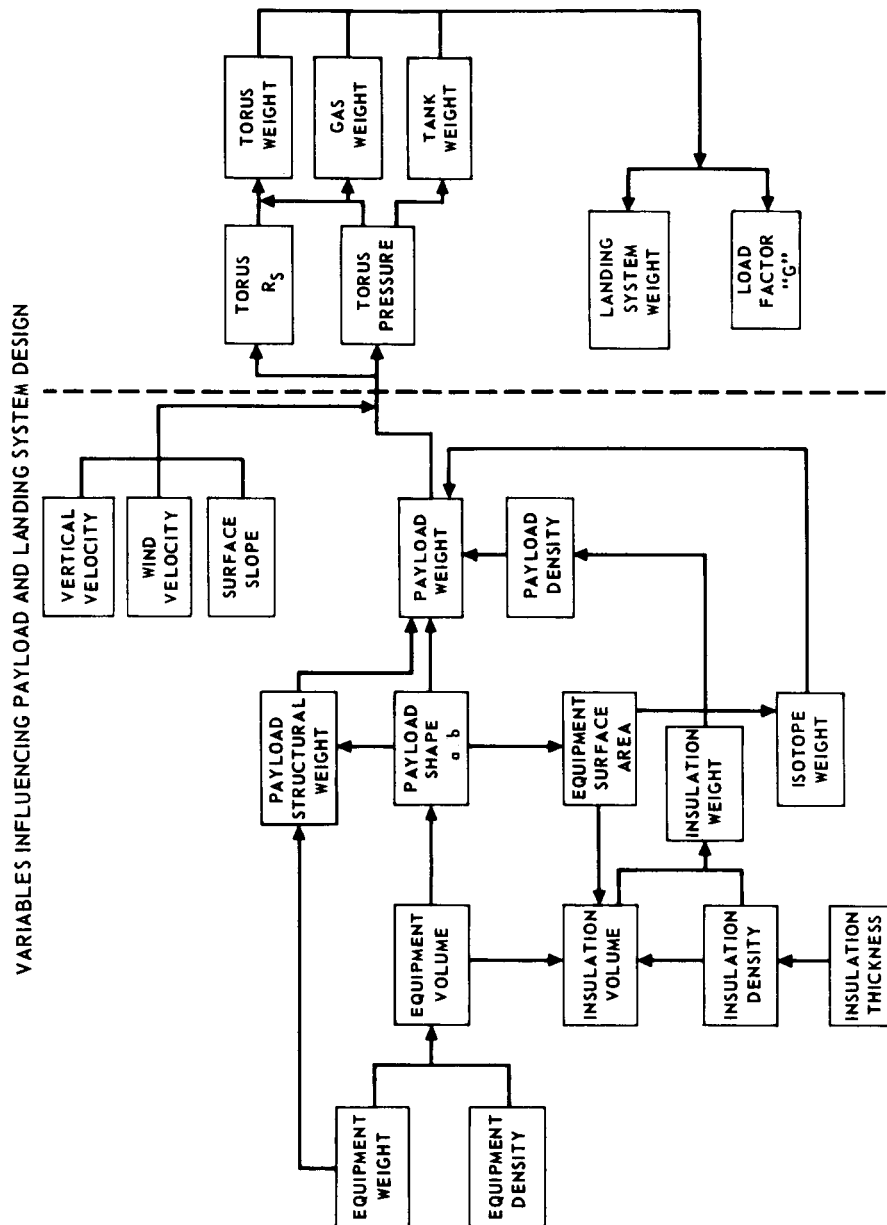
Dimensions X and Y are defined by Equations (7) and (9) respectively. Load stroke curves for parametric studies were obtained by multiplying the footprint area defined by Equation (18) by the associated torus pressure defined by Equation (10). The linear spring constant, K_F , is determined by equating the energy stored in the linear spring during a given stroke to the area under static load stroke curve to the same stroke of interest.

6.6 Lander Parametric Studies

6.6.1 PAYLOAD CONFIGURATION - Early in the study of inflatable torus landers, it was found that weight of landing system was quite sensitive to payload shape. Introducing a slight change in the ratio of payload diameter to payload height (a/b) produces a significant change in attenuator weight. Therefore, it was necessary to select a payload shape which represents a good compromise between landing system weight and equipment packaging requirements.

To aid in selecting payload configuration, a parametric study was conducted to determine the effects of equipment weight and density, payload geometry, and thermal control requirements on the landing system. Figure 6.6.1-1 is a flow diagram showing all variables which are influenced by or have an influence on payload shape. For example, shape of the payload package affects payload package surface area influencing weight of insulation and isotope heaters. Since the payload shape is dependent upon many variables, a computer program was written to aid in determining effect of these variables. Figure 6.6.1-2 shows the effect of payload dimensions a , b , and a/b , on the payload volume and surface area. As the value of a/b is increased along a constant volume line, surface area of the payload increases considerably. An increase in payload surface area requires additional isotope heaters and an increase in insulation. The influence of payload shape parameter a/b on landing system weight is shown in Figure 6.6.1-3. This figure shows that it is desirable to select a payload having a large value of a/b . Landing system weight decreases with large values of a/b because a larger percentage of torus radius is available for dissipating kinetic energy.

Design layouts were prepared to determine the influence of payload shape parameter (a/b) on packaging of equipment. In order to achieve good equipment packing densities and due to the height of some equipment, a reasonable value for a/b is 3. Figure 6.6.1-4 is a payload design layout showing typical equipment as listed in Figure 6.6.1-5. Equipment is packaged at a density of 80 lb/ft^3 using 80 percent of total available volume. Total payload density, including structure and thermal control, is 52.5 lb/ft^3 .



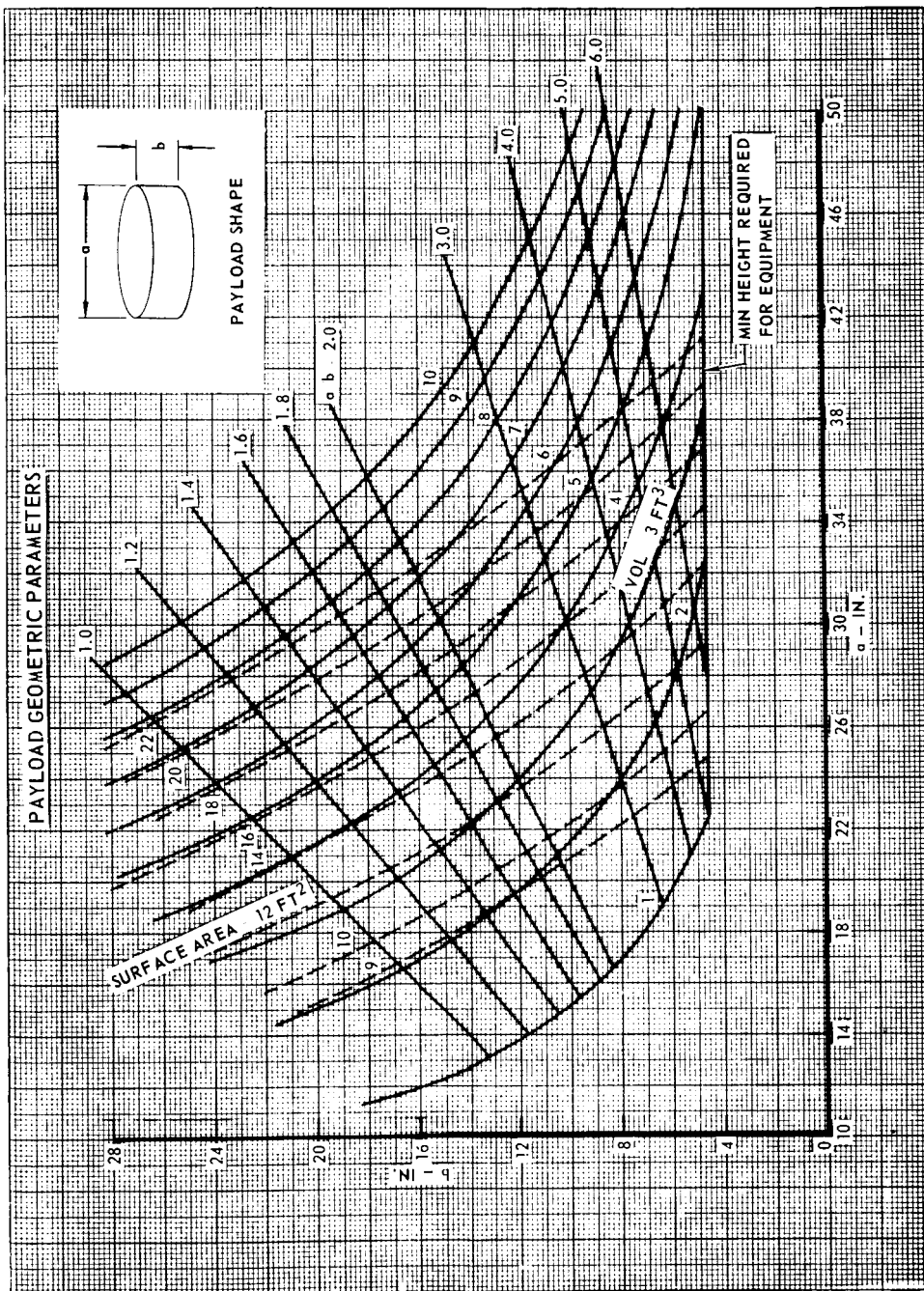
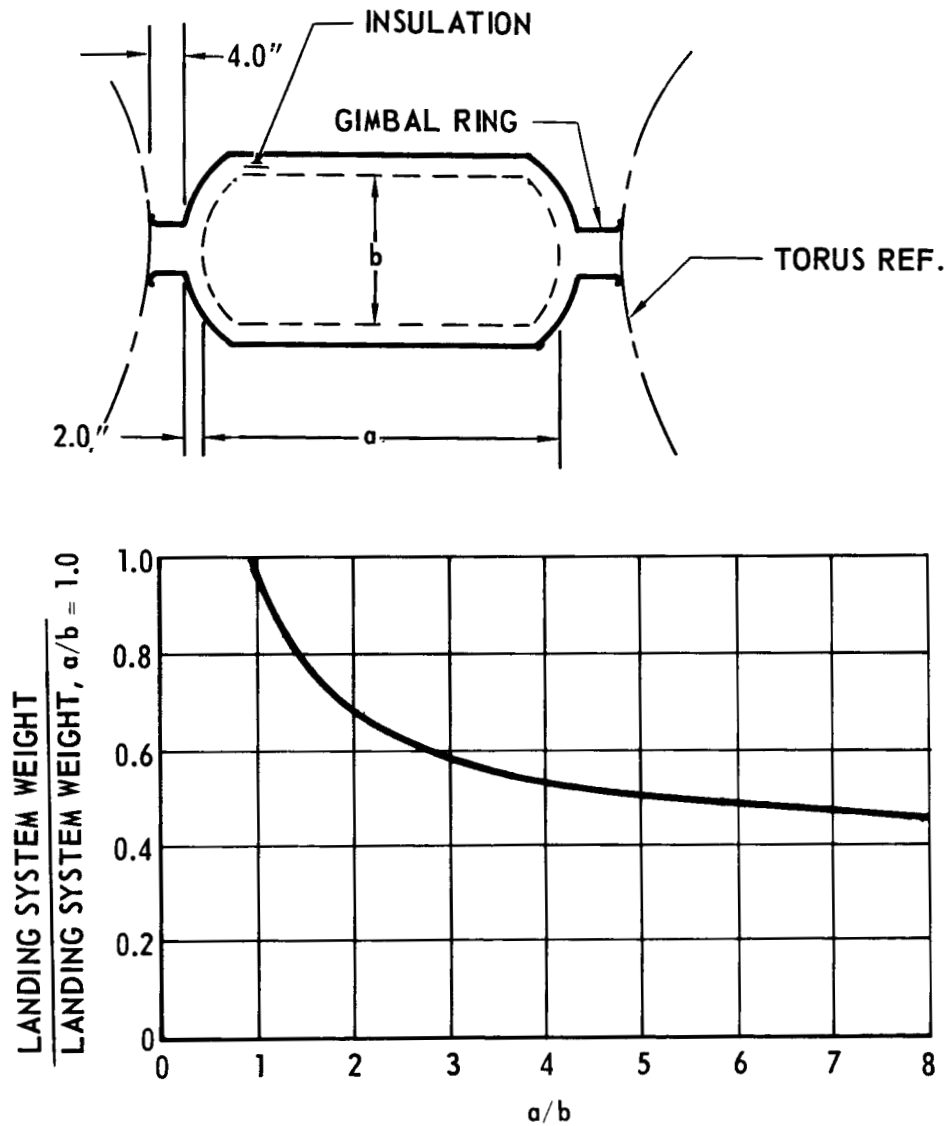


FIGURE 6.6.1-2

6.6-3

INFLUENCE OF PAYLOAD SHAPE ON LANDING SYSTEM WEIGHT



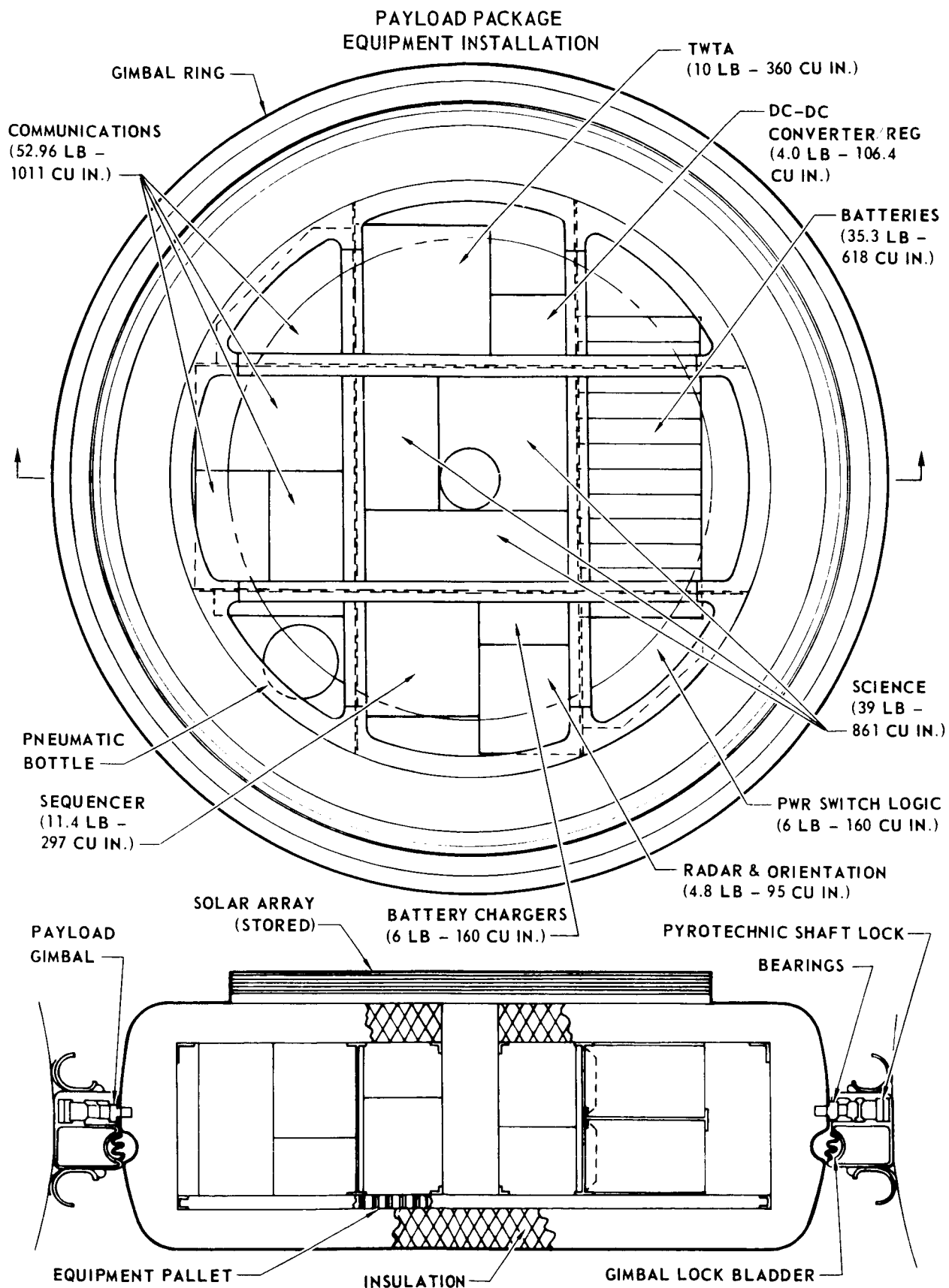


FIGURE 6.6.1-4

6.6-6

TYPICAL INTERMEDIATE LANDER EQUIPMENT

ITEM	VOLUME (IN. ³)	WEIGHT (LB)
SEQUENCER	297.0	11.4
COMMUNICATIONS	1 370.6	63.0
RADAR & ORIENTATION	95.0	4.8
ELECTRICAL POWER	1 042.8	76.5
SCIENCE	860.5	39.0
MECHANISMS	227.0	24.3
WIRING & MISC	1 058.0	56.0
SUBTOTAL EQUIPMENT	4 950.9	275.0
STRUCTURE	515.1	52.0
THERMAL CONTROL	5 540.0	49.0
TOTAL PAYLOAD	11 006.0	376.0

6.6.2 LANDING SYSTEM - Design of an interplanetary landing system is complicated by many severe environments experienced during its lifetime. Heat sterilization requirements and thermal environment experienced on the surface of Mars have the greatest effect on landing system design because of the use of non-metallic materials.

Since one of the basic missions of an interplanetary lander is to study the possibility of life forms existing on various planets, it is imperative that the landing system not carry any life forms which would contaminate the planet or nullify experiments. Since this requirement dictates that all components of the landing system must be terminally heat sterilized, selection of components is greatly affected. Thermal environments in addition to sterilization occurring during interplanetary cruise, entry, inflation, landing, and post landing, impose severe requirements for both high and low temperature capability. System components must sustain these temperature extremes for long periods of time along with the capability of changing from one extreme to the other in a very short time.

The vacuum of space also has a significant effect on landing system design. Some organic materials and composite materials are subject to outgassing and when combined with radiation usually lead to reduced flexibility and, in some cases, a decrease in mechanical properties.

6.6.2.1 Materials. - Selection of adequate materials for an inflatable lander requires close examination of candidate material properties.

Material properties considered include:

Strength	Density
Thermal Resistance	Sterilization Capability
Foldability	Abrasion Resistance
Permeability	Damping Characteristics
Adhesive Capability	Vacuum and Radiation Resistance
Puncture Resistance	

The requirement that all materials must be thermally sterilized is probably the major consideration that limits the selection of fabric materials

and elastomers for use in inflatable structures. Many organic materials possessing high strength to weight ratios are severely degraded during sterilization.

Flexibility and foldability are factors that must be considered, since the material will be stored in a deflated condition for a long period of time. After the material is subjected to severe environments of vacuum, radiation, and large temperature gradients, it must not contain cracks or adhere to itself. It must be sufficiently flexible at inflation temperatures to prevent failure due to rapid inflation.

Strength and density of materials are important in order to provide a lightweight attenuation system. Materials must retain satisfactory physical and mechanical properties after being subjected to several severe environments.

Abrasion resistance of either the cloth or the elastomer is considered, but is not a major factor in the selection of the materials. Abrasion of the torus surface is slight due to the low inflation pressures of the system.

Permeability of the cloth and elastomers is also considered of secondary importance since the length of time for complete inflation is relatively short. With the torus containing in excess of 1000 ft³ of gas at pressures of about 10 psig, no appreciable amount of gas escapes within the time required for full inflation. However, if the torus must remain inflated for extended surface operation, then leakage is very important.

Fabrics available for fabrication of the inflatable structure include those made from metal, ceramic, and organic fibers as shown in Figure 6.6.2-1.

Metal fabrics can be woven from 0.0015 inch diameter or larger monofilament wire in almost any weave desired. Woven metal fabrics produced from monofilament wire have low flexibility and high porosity. These properties can be improved, however, by weaving the fabric from stranded yarns of fine superalloy.

Strength to weight ratio of candidate organic fabrics is far superior to metal fabrics. However, metal fabrics can withstand much higher temperatures and are more resistant to abrasion. In addition, since the permeability

CANDIDATE FABRICS FOR TORUS

ORGANIC	CERAMIC	METALLIC
<p>POLYOLEFINS</p> <p>POLYETHYLENE</p> <p>POLYPROPYLENE</p> <p>POLYAMIDE</p> <p>NYLON</p> <p>HT-1 ("NOMEX")</p> <p>POLYESTER</p> <p>DACRON</p> <p>POLYBENZIMIDAZOLE (PBI)</p> <p>PARTIALLY CARBONIZED</p> <p>CARBON</p> <p>GRAPHITE</p>	<p>FIBERGLASS</p> <p>"E" GLASS</p> <p>S-994 GLASS</p> <p>YM-31A GLASS</p> <p>HOLLOW GLASS</p> <p>LEACHED FIBERGLASS</p> <p>QUARTZ FIBERS</p>	<p>LOW CARBON STEEL</p> <p>300 SERIES STAINLESS STEEL</p> <p>WROUGHT SUPERALLOYS</p> <p>ALUMINUM AND ALUMINUM ALLOY</p> <p>TITANIUM AND TITANIUM ALLOY</p>

of the metal fabrics is high, it is necessary to use an internal liner in the torus for gas retention.

Storage volume of the deflated structure, when produced from metallic fabrics rather than organic fabrics, is considerably greater due to the poor foldability of the metallic fabrics and the addition of a liner. Metallic fabric structure is heavier and takes up more space in the aeroshell than the organic fabric structure. Therefore, metal fabrics are not selected unless the stringent requirements of thermal and space environments exceed the limits of organic fabrics.

Ceramic fabrics considered included those constructed from fiberglass and quartz fibers. These materials easily withstand sterilization, however, they are not satisfactory due to their brittleness and poor abrasion resistance. These fibers are easily scratched which may eventually lead to fiber failure.

Most organic fabric materials were eliminated due to severe degradation of physical and mechanical properties during thermal sterilization. Candidate materials are nylon, HT-1 (a high temperature polyimide known by its trade name, Nomex), and Dacron (a polyester fiber).

Nylon is seriously degraded by thermal sterilization and as a result was eliminated from further consideration. The average strength loss of Dacron after sterilization and 30-day vacuum exposure was about 20 percent. Since test data indicated continuing material degradation due to vacuum soaking throughout the 30-day test period, it is doubtful that Dacron would be acceptable after 230 days in a vacuum.

The leading candidate material is HT-1 (Nomex) with average strength losses resulting from both sterilization and vacuum exposures of less than 5 percent. At room temperature, the strength of Nomex is inferior to nylon and Dacron, however, when Dacron was tested at 200°F, its strength to weight ratio was found to be inferior to Nomex. Therefore, due to the requirement for sterilization, Nomex is preferred for inflatable structure. Pertinent factors influencing fabric selection are summarized in Figure 6.6.2-2.

The fabric selected for the inflatable structure is coated with an elastomer to seal the structure for gas retention and to provide abrasion and

FABRIC SELECTION SUMMARY

ORGANIC

NYLON

- HIGH STRENGTH TO WEIGHT RATIO AT ROOM TEMPERATURE
- SERIOUS DEGRADATION AFTER THERMAL STERILIZATION

DACRON

- 20% STRENGTH DEGRADATION AFTER THERMAL STERILIZATION AND VACUUM EXPOSURE
- STRENGTH TO WEIGHT RATIO INFERIOR TO NOMEX AT 200°F

NOMEX

- ONLY SLIGHT DEGRADATION AFTER STERILIZATION AND VACUUM EXPOSURE
- RETAINS MECHANICAL PROPERTIES AT ELEVATED TEMPERATURES

CERAMIC

- ELIMINATED DUE TO THEIR BRITTLINESS AND POOR ABRASION RESISTANCE

METALLIC

- CAN WITHSTAND STERILIZATION TEMPERATURES
- GOOD ABRASION RESISTANCE
- HIGH DENSITY
- VERY HIGH PERMEABILITY
- LOW STRENGTH TO WEIGHT RATIO

puncture protection to the basic fabric. Low and elevated temperature requirements greatly restrict the choice of elastomers also. It appears that within the present state-of-the-art, a silicone rubber compound of the methyl-phenyl type is the best selection to meet all criteria. Candidate elastomers are compared in Figure 6.6.2-3.

6.6.2.2 Inflation systems. - Three basic inflation systems were considered for the intermediate lander. These systems are stored pressurized gas, cool gas generator, and hot gas generator. To select the proper inflation system, considerations were given to the following items:

Simplicity and Reliability	Ambient Conditions
Inflated Volume	Transient Temperatures & Pressures
Inflated Pressure	Effect of Sterilization
Time Required for Inflation	System Weight and Volume
Leakage	Packaging
Cost	

A cool gas generator consists of a gas stored at high pressure and a hot gas propellant. For pressurization of the torus, the hot propellant gas is mixed with the stored gas and injected into the storage volume resulting in a combined system which has a high ratio of gas volume to storage volume resulting in a lightweight design. Inflation rate is very rapid regardless of temperatures. Cool gas from storage and hot gas from propellant are mixed in proper proportions resulting in a gas temperature that is not detrimental to the fabric.

The hot gas generator utilizes exhaust products from burning of a solid or liquid propellant to achieve rapid inflation. Also, since the gas is delivered at high temperatures, it must be delivered at a sufficiently high pressure to allow for subsequent cooling. These high pressures and high temperatures are harmful to the fabric and elastomers of the inflatable structure.

The stored pressurized gas system was chosen for the parametric studies primarily because it is simple, highly reliable, and it is competitive in weight. This system consists of a high ratio of gas volume to storage volume.

CANDIDATE ELASTOMERS FOR INFLATABLE TORUS FABRICATION

PROPERTIES	NATURAL RUBBER	BUTYL	BUNA-N	NEOPRENE	HYPALON	POLY-URETHANE	SILICONE
TENSILE STRENGTH (PSI)	1125	2150	1250	1450	1500	5425	525
SHORE HARDNESS	30-90	40-75	40-95	30-95	50-85	60-90	25-85
SPECIFIC GRAVITY	.93	.92	1.00	1.25	1.35	1.27	.98
VULCANIZING	EXCEL	GOOD	EXCEL	EXCEL	GOOD	EXCEL	EXCEL
ADHESION TO METAL	EXCEL	GOOD	EXCEL	EXCEL	GOOD	GOOD	FAIR
ADHESION TO FABRICS	EXCEL	GOOD	GOOD	EXCEL	GOOD	GOOD	FAIR
TEAR RESISTANCE	GOOD	GOOD	FAIR	GOOD	GOOD	EXCEL	POOR
ABRASION RESISTANCE	VERY GOOD	GOOD	GOOD	GOOD	GOOD	EXCEL	POOR
AIR PERMEABILITY (180°F) CC/SEC./CM. ² x 10 ⁻⁷	3.5	.32	1	.98	.73	.97	44
TEMPERATURE RANGE (°F)	-75 TO +200	-75 TO +300	-65 TO +275	-65 TO +250	-55 TO +275	-65 TO +250	-150 TO +500

*AFTER HEAT AGING IN N₂

High pressure gas is released upon command through a pressure or flow device, fed into a manifold around the gimbal ring, and expanded into the torus. The torus must be fully inflated during parachute descent requiring pressurization within 40-50 seconds. This rapid expansion of most gases requires thermal energy to bring them to full inflation efficiency. However, by using helium as the pressurant, thermal energy is not required. Tank weight and size are based on storing helium at 5000 lb/in² in a titanium spherical tank. After torus inflation, the storage tank is released with the parachute to eliminate attenuating this additional energy at landing.

Pertinent features of inflation systems are summarized in Figure 6.6.2-4.

6.6.2.3 Study results. - In the preceding paragraphs, various components of the torus landing system were discussed and preferred approaches selected. These components include the inflation system and materials for the torus. In addition, analytical methods and computer programs for determining landing system weight and performance were presented.

A stored pressurized gas system using helium was selected in Section 6.6.2.2. This system is comprised of the gas and the pressure tank. Associated valves and lines are assumed to be a part of the payload. Tank weight is obtained from Equation (14) (Section 6.5.2.2) using titanium alloy 6lA-4V as the tank material and a factor of safety of 2.22. This titanium alloy has the following properties:

$$F_{TU} = 160\,000 \text{ lb/in}^2$$

$$\rho = 0.160 \text{ lb/in}^3$$

When the lander is separated from parachute, the pressure tank remains with the parachute. Therefore, the tank is not included in landed mass although it is considered part of landing system.

Nomex cloth was selected in Section 6.6.2.2 for the torus material and is used in parametric studies. Nomex has a strength to weight ratio of 1 000 000 $\frac{\text{lb/in}}{\text{lb/in}^2}$. Weight of elastomer used to seal the Nomex and provide

INFLATION SYSTEMS

STOWED PRESSURIZED GAS

- **HIGH RATIO OF GAS VOLUME TO STORAGE VOLUME**
- **RAPID INFLATION**
- **COOL TEMPERATURES DUE TO EXPANSION OF SOME GASES**
- **SIMPLE AND RELIABLE**

COOL GAS GENERATOR

- **HOT PROPELLANT GAS IS MIXED WITH STORED GAS**
- **RAPID INFLATION**
- **LIGHTWEIGHT**
- **SIMPLE**

HOT GAS GENERATOR

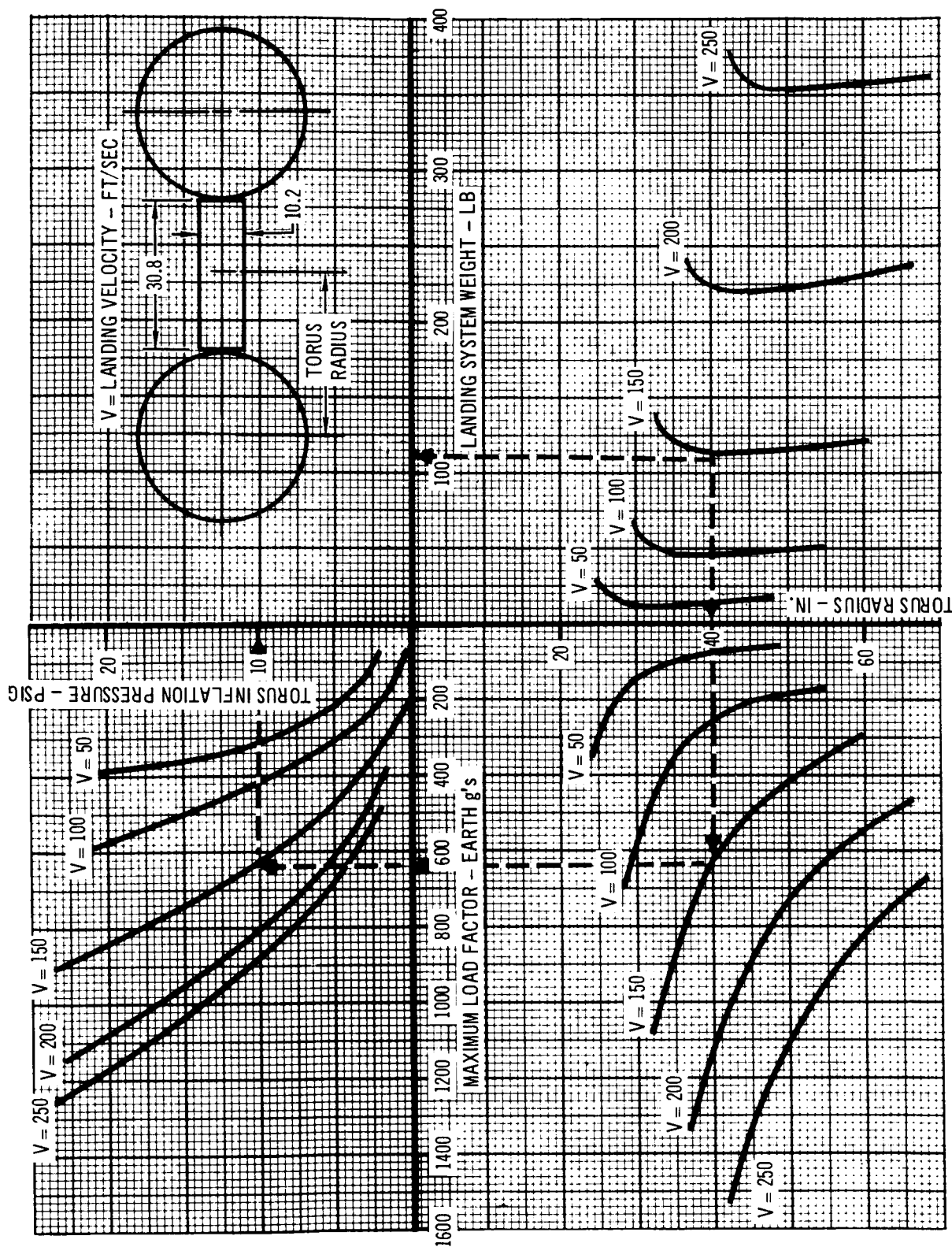
- **HOT PROPELLANT GAS IS USED FOR INFLATION**
- **HOT GAS MAY BE HARMFUL TO MATERIALS**
- **LIGHTWEIGHT**
- **RAPID INFLATION**

scuff resistance is assumed to be equal to cloth weight. A seam efficiency factor of 0.85 is used to account for weight of material overlap at seams.

Landing system design parameters for 100, 200, 300 and 400 pound payload weights are shown in Figure 6.6.2-5 through 6.6.2-8. These curves define landing system weight, maximum load factor, torus radius and inflation pressure as a function of landing velocity. Using these curves it is possible to select torus geometry and inflation pressure which result in minimum landing system weight. For example, on Figure 6.6.2-5, the dashed line defines a minimum weight landing system capable of landing a 100 pound payload at 150 ft/sec. Landing system weight is 115 pounds; lander radius is 40 inches; maximum load factor is 620 Earth g's; and inflation pressure is 10 psig. It is important to note that load factor could be reduced by using a larger lander radius with a slight increase in landing system weight. Minimum landing system weight obtained from Figures 6.6.2-5 through 6.6.2-8 are plotted in Figure 6.6.2-9. as a function of landing velocity and payload weight.

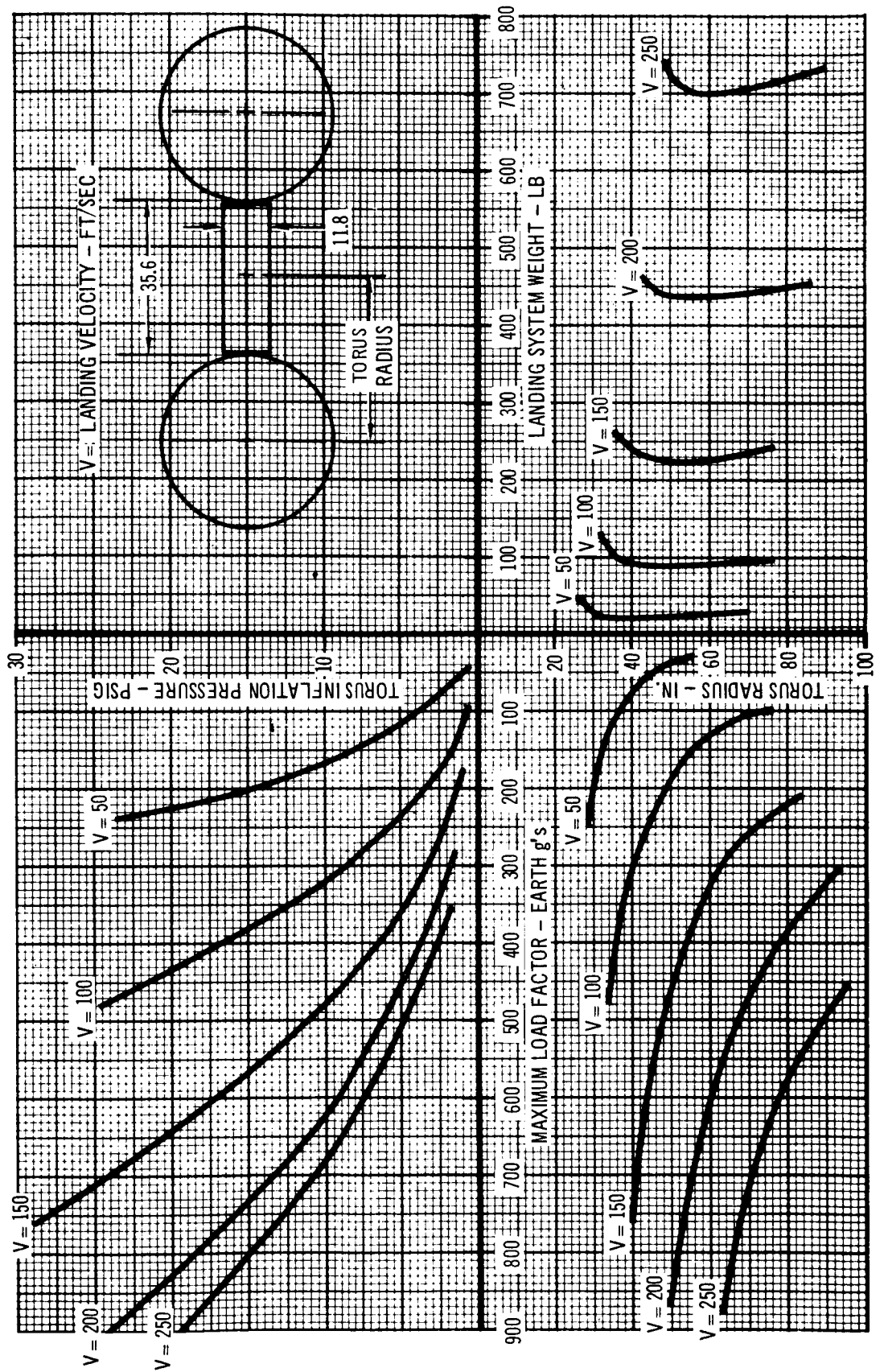
INFLATABLE TORUS LANDING SYSTEM DESIGN PARAMETERS

PAYLOAD WEIGHT = 100 LB



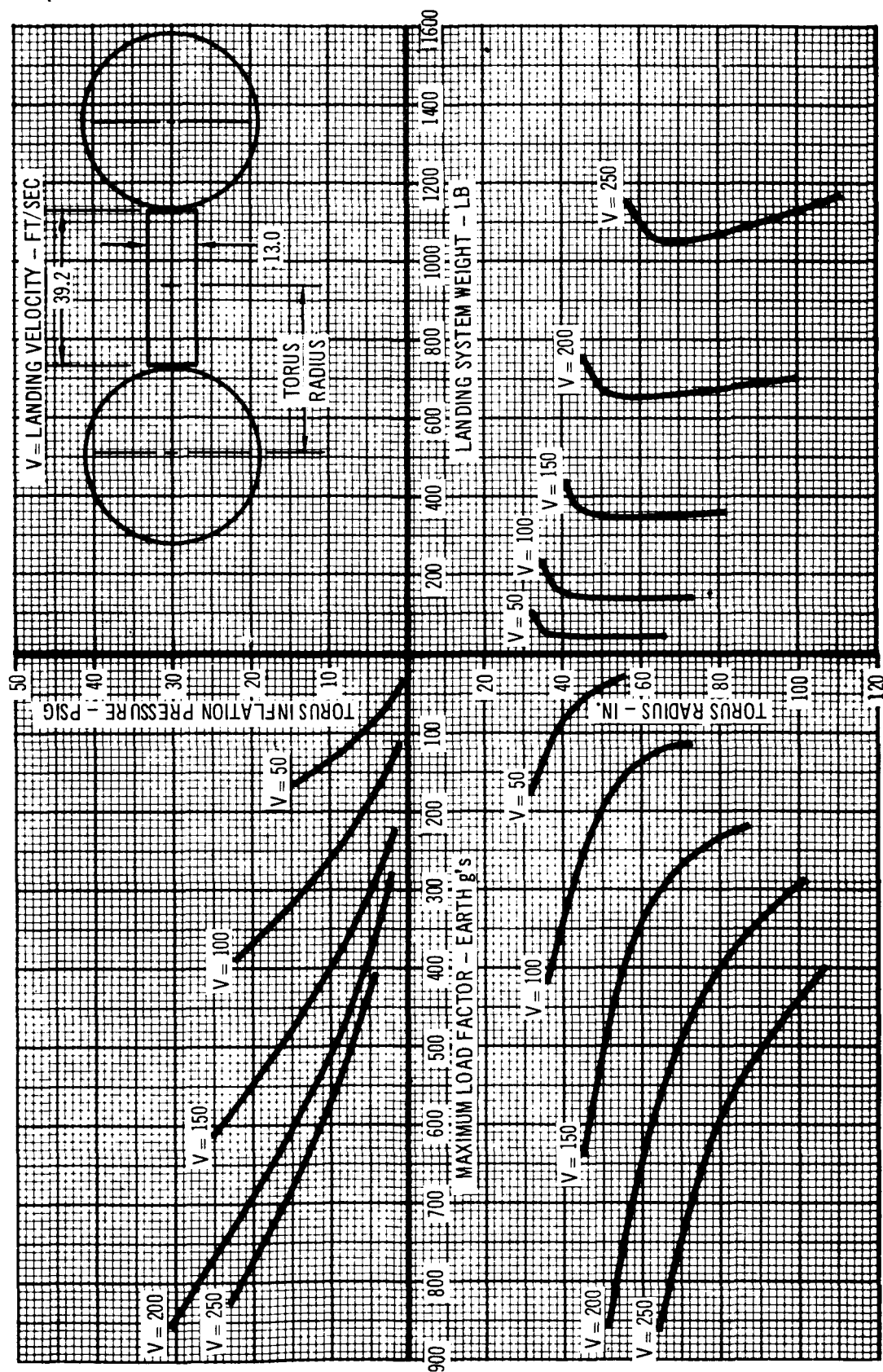
INFLATABLE TORUS LANDING SYSTEM DESIGN PARAMETERS

PAYLOAD WEIGHT = 200 LB



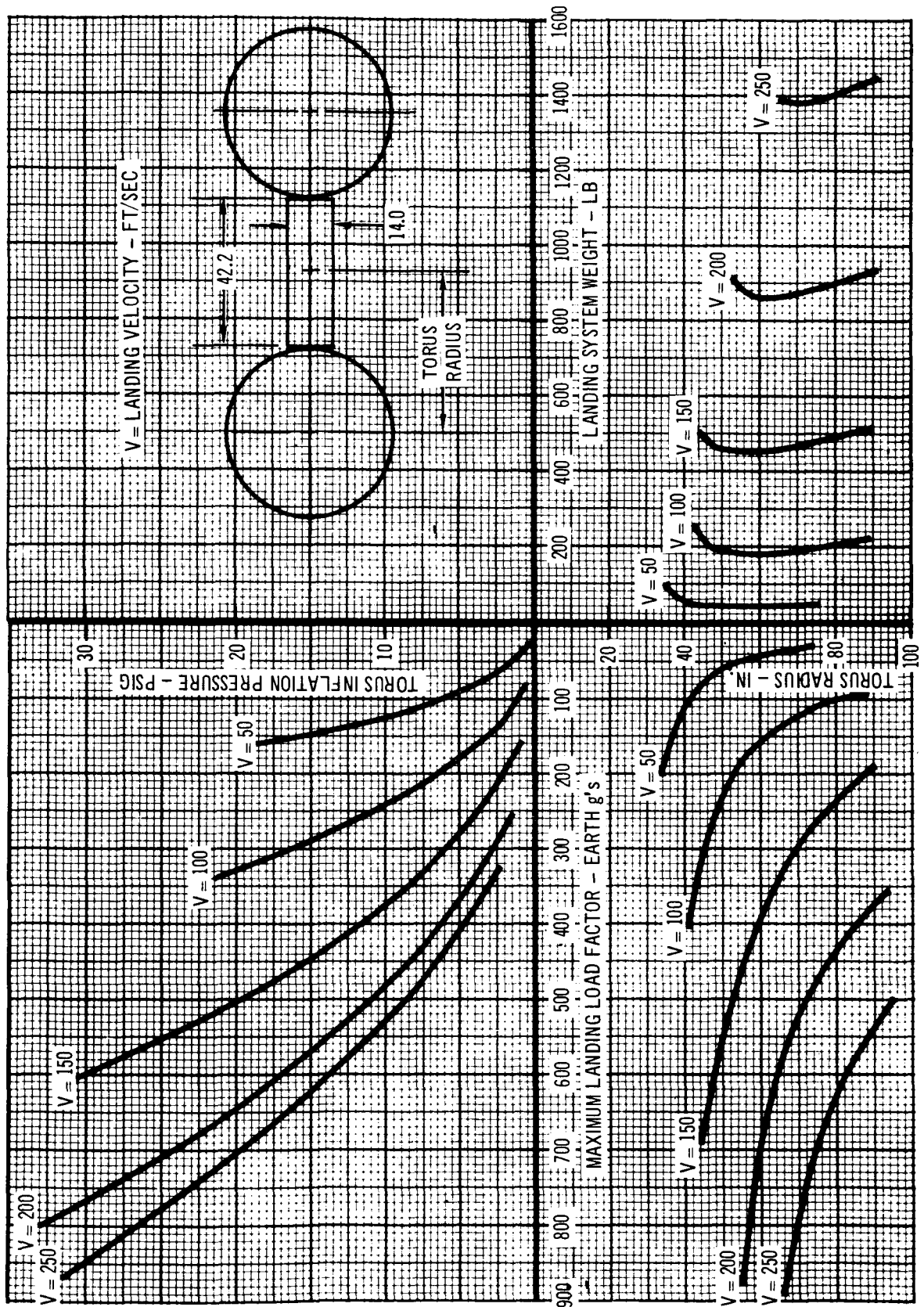
INFLATABLE TORUS LANDING SYSTEM DESIGN PARAMETERS

PAYLOAD WEIGHT = 300 LB

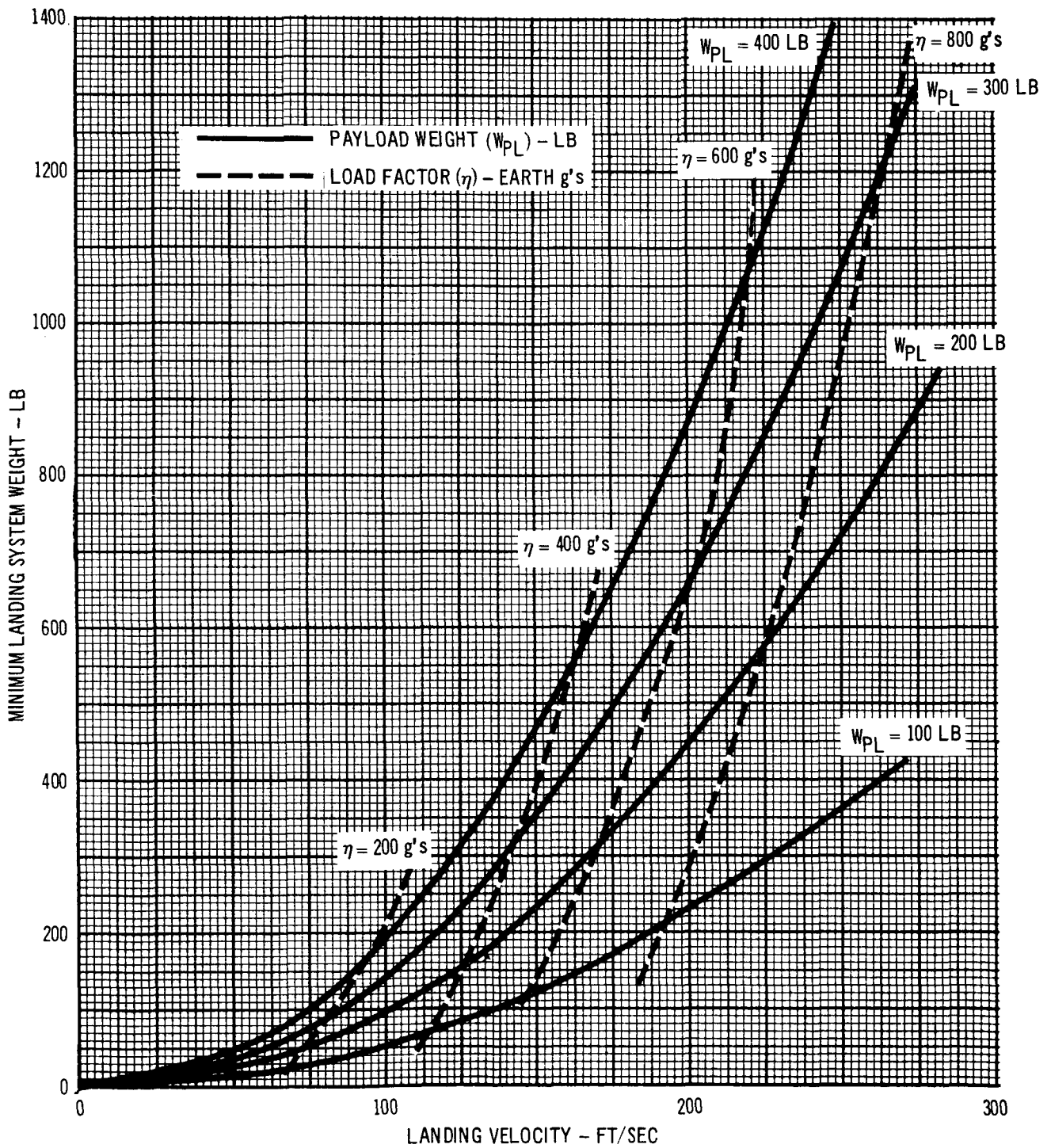


INFLATABLE TORUS LANDING SYSTEM DESIGN PARAMETERS

PAYLOAD WEIGHT = 400 LB



EFFECTS OF LANDING VELOCITY AND PAYLOAD WEIGHT ON LOAD FACTOR AND MINIMUM LANDING SYSTEM WEIGHT



6.7 Additional Design Considerations

6.7.1 PAYLOAD ATTACHMENT - Three concepts for attaching payload to torus were studied. These concepts were: fixed payload, single gimballed payload, and double gimballed payload.

The fixed payload concept attaches the payload package directly to the torus. Since the torus is bi-stable, provisions for instrument deployment consist of one of the following arrangements: 1) Dual experiments and equipment, 2) Individual gimbaling of selected experiments requiring orientation, 3) Use of a flip-over mechanism to right the lander in case it comes to rest upside down. This latter concept allows single instruments and a single solar array.

A single gimballed payload concept utilizes one gimbal ring located around the payload circumference as shown in Figure 6.6.1-4. The payload is mounted in a single axis trunion which allows the entire payload to rotate. A gimbal lock bladder installed around the periphery of the payload distributes impact loads to the gimbal ring and into the torus landing system. This concept permits installation of single fixed instruments and a single solar array. The lock bladder is inflated prior to entry and vented after landing. After the payload has rotated to achieve an upright position, trunion locks are engaged to rigidize the gimbal mechanism.

The double gimballed payload concept provides the payload with two axes of rotation thus permitting alignment to local gravity vector. This concept is similar to the single gimbal concept with the exception of another trunion axis located in an inner gimbal ring. The inner gimbal and payload are supported on precision bearing trunions during leveling. Trunions are in elastic mounts so that they do not carry any appreciable load during impact.

The weight estimated for the single gimbal concept was used in parametric studies.

6.7.2 REBOUND DAMPING - The inflatable landing system stores a large amount of energy during landing which unless dissipated, causes considerable rebound. Examination of test data given in Appendix A shows that the average

velocity at second impact was about 73 percent of initial impact velocity for flat landing and about 88 percent for end landings.

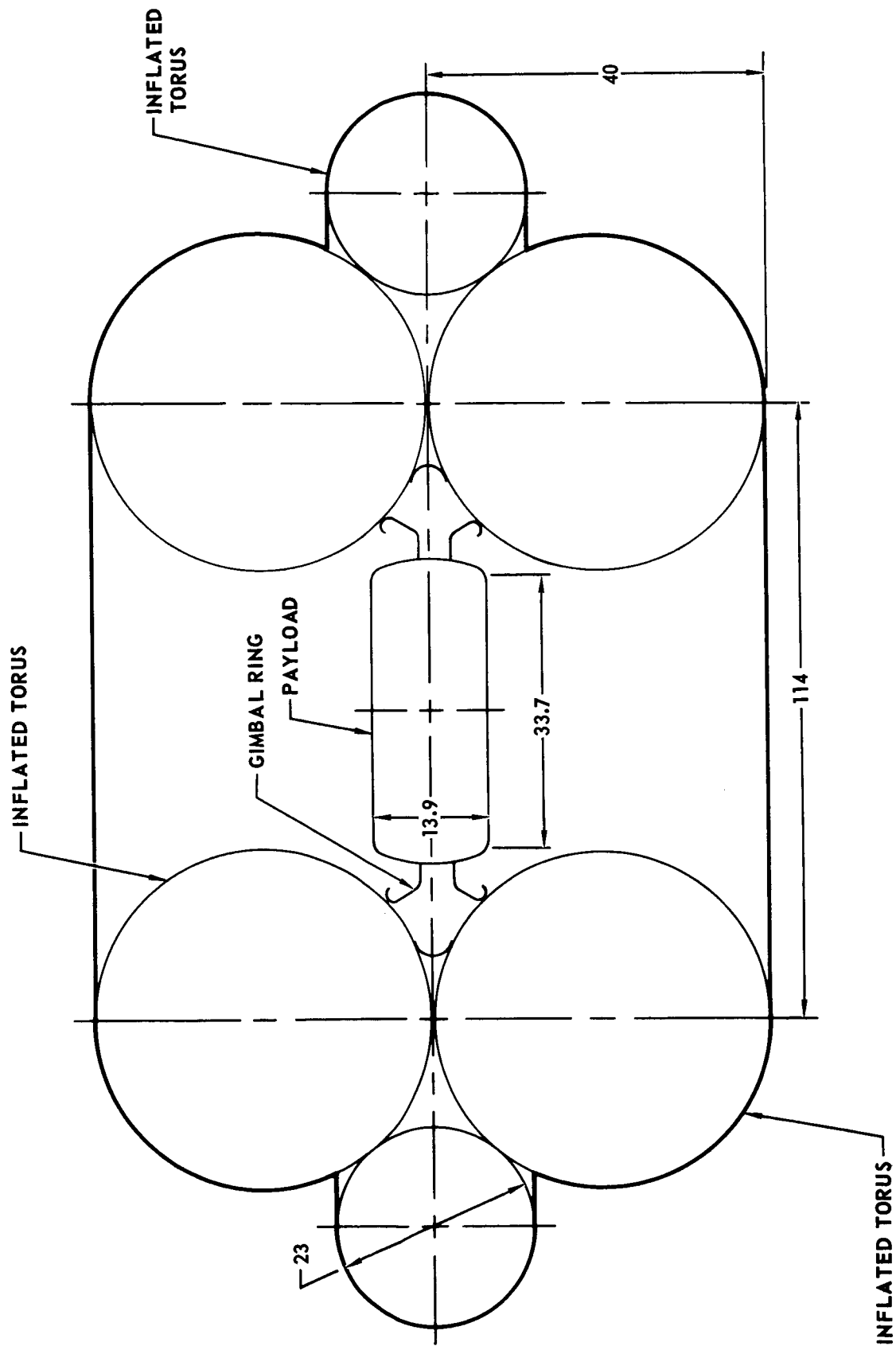
Rebound damping of a nonventing system is dependent upon internal working of the fabric and gas. Previous limited drop testing of the model indicated that energy losses for oblique impacts may be significantly higher than those occurring for flat or end landing. Thus, it may be desirable to select a landing orientation which will insure an oblique landing initially. Further tests and analyses are needed to confirm this however.

Damping by external venting of the torus is accomplished by using either fixed or variable orifices. The fixed orifice concept is activated by an impact switch which allows pressure relief at instant of impact. The variable orifice is a method which regulates internal pressure by allowing the orifice area to increase as the internal pressure increases, thus approaching ideal orifice flow characteristics. Normally, performance is increased by utilizing variable orifices instead of fixed orifices. However, because of low atmospheric pressure on Mars, torus pressures do not increase significantly during landing thus the advantage offered by variable orifices is reduced.

Rebound damping of the landing system can also be accomplished by internal compartmentation with permeable dividers, fixed orifices, or by controlled venting.

6.7.3 ALTERNATE LANDING SYSTEMS - Several inflated landing systems including inflatable single sphere, multiple spheres, single torus, triple torus, and multiple torus were studied. As a result of these studies, the triple torus configuration shown in Figure 6.7.3-1 was chosen as an alternate. This configuration consists of three inflated tori surrounding the payload. The two large tori are designed to attenuate the payload while the small torus is used to prevent the lander from coming to rest on edge. Payload attachment is similar to the single torus. The primary advantage of the triple torus configuration is the capability for deflating the upper torus thus greatly increasing space available for atmospheric sensor deployment. Although the triple torus landing system is slightly lighter in weight than the single torus this advantage is overshadowed by the complications of additional manifolds and valves in the inflation system.

TRIPLE TORUS GEOMETRY



6.8 Conclusions

Inflatable torus landing systems are feasible for the range of landing velocities and payload weights considered. Reasonable landing system weights are achieved for payload weights up to 400 lb and landing velocities less than about 150 ft/sec. At higher velocities, landing system weight increases rapidly. However, if minimizing landing load factors is a serious requirement, then the inflatable torus concept may be desirable for velocities above 150 ft/sec also. Methods for reducing rebound should be studied and verified by test so that the time from first impact to rest can be minimized.

Payload strokes and accelerations can be determined analytically for flat landings using a two degree of freedom model. Parameters used in the analytical model were defined and verified by test. In general, strokes required for end landings are approximately twice the strokes required for flat landings. However, accelerations experienced by payload during an end landing were about one-half those experienced during flat landings.

APPENDIX A - TEST RESULTS

Static and dynamic tests of a model lander were conducted to obtain empirical data for lander parametric studies. The test model, shown in Figure A-1, consists of an inflated torus continuously attached to an inner payload ring. Maximum diameter of model is 42.78 inches and payload diameter is 13.14 inches.

Results of static and dynamic tests are presented in this section.

Static Tests - Static test set-up is shown in Figure A-2 for flat and end tests. The torus rested on a flat rigid surface and load was applied to the payload ring. All tests were conducted in ambient conditions and internal torus pressure was measured throughout the test. Payload displacement was read from a scale and pointer device. The test schedule is also shown in Figure A-2. Flat and end loading static test results are shown in Figures A-3 and A-4 respectively.

Dynamic Tests - Dynamic tests of the torus were conducted by dropping the model as shown in Figure A-5. Tests were conducted in the Zero Gravity Research Facility at the NASA Lewis Research Center in Cleveland, Ohio. The drop test schedule is shown in Figure A-6.

For flat landings, the torus was guided by a single cable stretched from the top of the chamber to the landing surface. The lower portion of the cable was calibrated so that payload stroke could be read from high-speed films. Timing marks were placed on films so that landing velocity could be determined also. Three high speed cameras were located at the landing surface. One camera focused directly on the cable for stroke and velocity measurements while the other two, spaced 90 degrees apart, recorded lander orientation during impact. Internal pressure was monitored throughout each test by means of a pressure transducer located on the payload. Three single-axis accelerometers were used to measure accelerations in three orthogonal directions during impact. For many of the drops, second, third, and sometimes fourth impact data were obtained. Results of flat landing tests are presented in Table A-1.

TEST MODEL DESCRIPTION

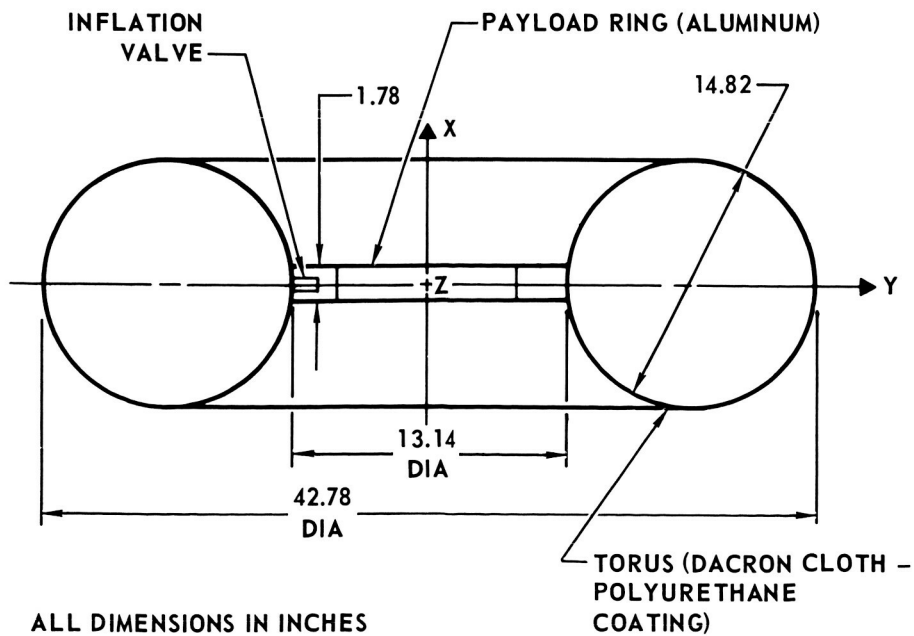
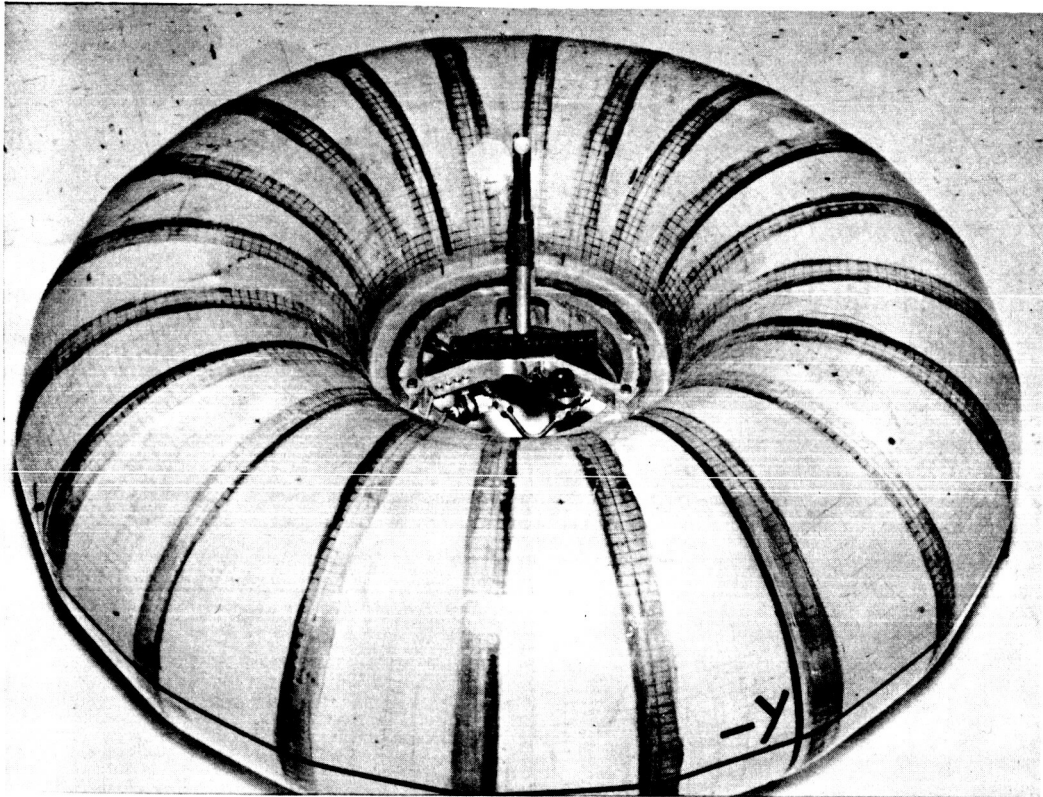
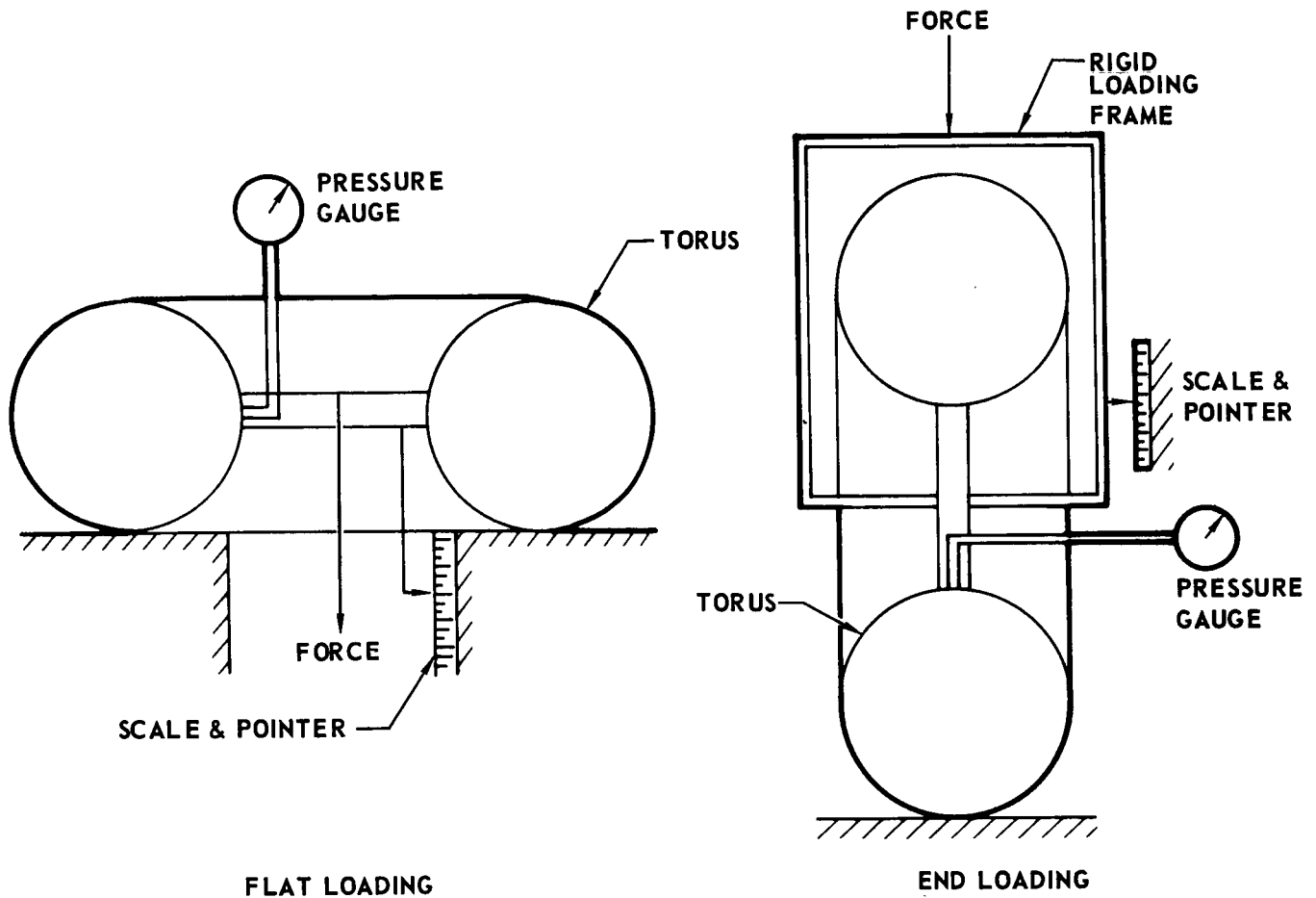


FIGURE A-1
A-2

STATIC TEST SET-UP



SCHEDULE

TEST NUMBER	LANDER ORIENTATION	INITIAL PRESSURE (PSIG)	MAXIMUM PAYLOAD STROKE (IN.)
1	FLAT	2.0	3.0
2	FLAT	4.0	4.0
3	FLAT	6.0	5.0
4	END	2.0	5.0
5	END	4.0	6.5

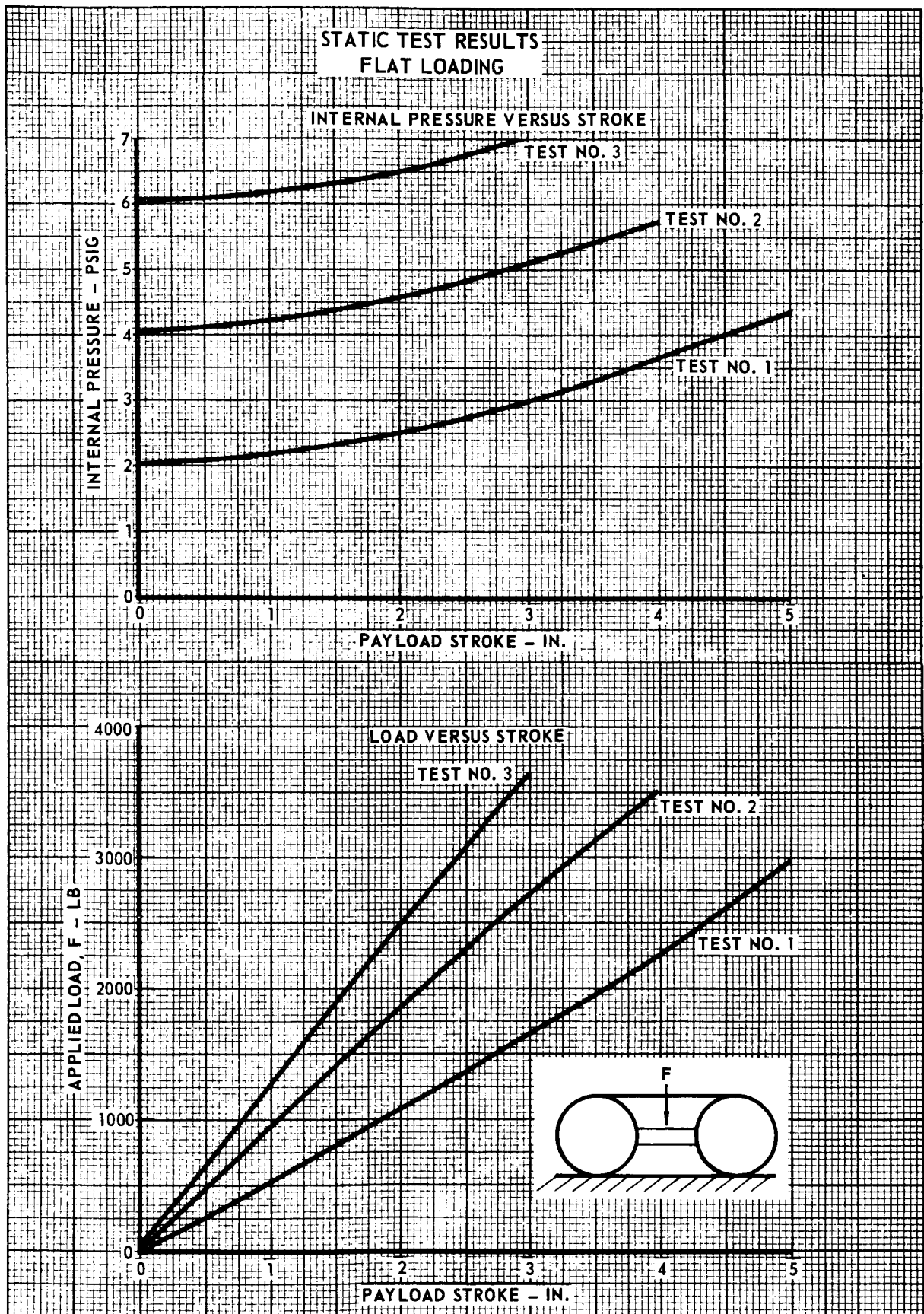


FIGURE A-3

A-4

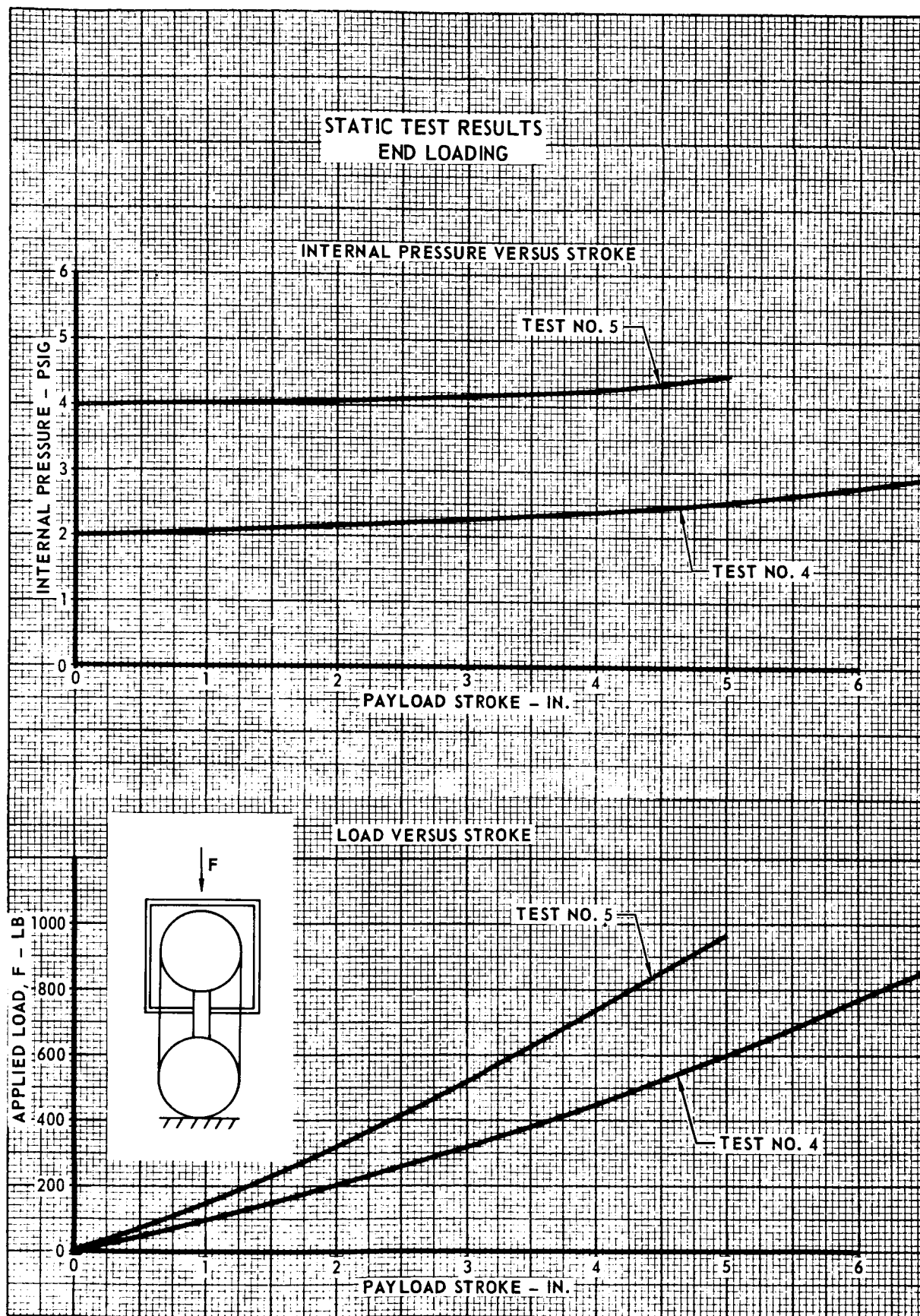
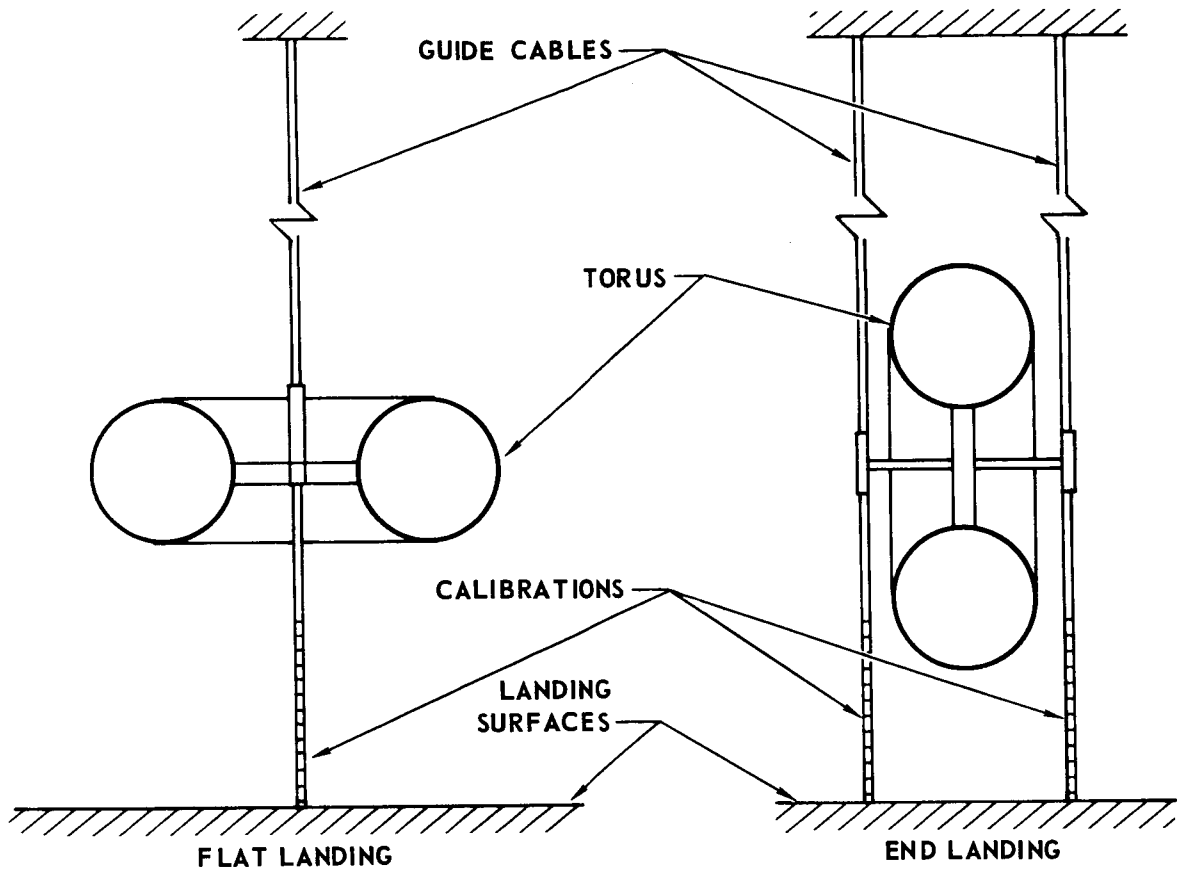


FIGURE A-4
A-5

DYNAMIC TEST SET-UP



INSTRUMENTATION	PURPOSE
3 - ACCELEROMETERS	DETERMINE ACCELERATIONS IN THREE DIRECTIONS
3 - HIGH SPEED CAMERAS	DETERMINE PAYLOAD STROKE, LANDING VELOCITY AND LANDER ORIENTATION
1 - PRESSURE TRANSDUCER	DETERMINE TORUS PRESSURE AT IMPACT

TORUS DYNAMIC TEST SCHEDULE

TEST NUMBER	LANDING ATTITUDE	INFLATION PRESSURE (PSIG NOMINAL)	PAYLOAD WEIGHT (LB)	DROP HEIGHT (FT)
1	FLAT ↓ FLAT END ↓ END	2.0	11.0	25.0
2		2.0 ↓ 2.0	4.1	25.0
3			7.5	25.0
4			7.5	25.0
5			7.5	6.2
6			4.1	6.2
7			11.0	6.2
8			4.1	39.0
9		4.0	7.5	56.0
10		4.0 ↓	4.1	56.0
11			11.0	56.0
12		4.0 ↓	7.5	76.0
13			4.1	99.5
14		6.0	7.5	56.0
15		6.0 ↓	4.1	56.0
16			7.5	99.5
17		6.0	4.1	155.0
18	FLAT END ↓ END	4.0	4.4	56.0
19		4.0	4.4	99.5
20		6.0	4.4	56.0
21		6.0 ↓	4.4	99.5
22			4.4	155.0
23		6.0 ↓	7.8	56.0
24			7.8	99.5

TABLE A-1
MODEL DYNAMIC TEST RESULTS
FLAT LANDING

TEST NUMBER	IMPACT NUMBER	PAYLOAD WEIGHT (LB)	INFLATION PRESSURE (LB/IN ²)	LANDING VELOCITY (FT/SEC)	MAXIMUM PAYLOAD STROKE (IN.)	MAXIMUM LOAD FACTOR ON PAYLOAD (EARTH g'S)		
						n _z	n _y	n _x
1	1	11.0	2.0	36	3.8	17	32	134
1	2	11.0	2.0	26	3.1	13	6	105
2	1	4.1	2.0	39	2.9	24	8	252
2	2	4.1	2.0	23	2.0	5	26	141
3	1	7.5	(1)	(1)	(1)	(1)	(1)	159
3	2	7.5	(1)	(1)	(1)	(1)	(1)	(1)
4	1	7.5	2.1	39	3.7	18	11	177
4	2	7.5	2.1	34	3.1	10	8	164
5	1	7.5	2.1	19	1.8	22	2	(1)
5	2	7.5	2.1	15	1.5	7	9	(1)
5	3	7.5	2.1	12	1.2	12	9	(1)
5	4	7.5	2.1	8	0.9	13	6	47
6	1	4.1	2.1	20	1.5	25	20	125
6	2	4.1	2.1	14	1.0	17	9	83
6	3	4.1	2.1	7	0.6	15	3	45
7	1	11.0	2.1	19	2.0	24	17	82
7	2	11.0	2.1	17	1.8	18	13	72
8	1	4.1	2.1	50	4.0	13	13	289
8	2	4.1	2.1	32	2.4	18	15	206
9	1	7.5	3.8	60	4.3	16	17	365
9	2	7.5	3.8	51	3.4	24	22	322
10	1	4.1	3.8	60	3.7	3	11	487
10	2	4.1	3.8	40	2.3	5	9	325
10	3	4.1	3.8	27	1.5	3	22	250
10	4	4.1	3.8	18	1.0	2	13	187

NOTE: (1) NO DATA OBTAINED

TABLE A-1 (Continued)
MODEL DYNAMIC TEST RESULTS (Continued)
FLAT LANDING

TEST NUMBER	IMPACT NUMBER	PAYLOAD WEIGHT (LB)	INFLATION PRESSURE (LB/IN ²)	LANDING VELOCITY (FT/SEC)	MAXIMUM PAYLOAD STROKE (IN.)	MAXIMUM LOAD FACTOR ON PAYLOAD (EARTH g'S)		
						n _z	n _y	n _x
11	1	11.0	3.8	60	5.2	21	18	295
11	2	11.0	3.8	53	4.4	17	19	265
11	3	11.0	3.8	46	3.8	12	18	250
12	1	7.5	3.8	70	5.2	18	24	425
12	2	7.5	3.8	57	4.2	13	26	362
12	3	7.5	3.8	46	3.7	12	12	325
13	1	4.1	3.8	80	5.3	14	9	642
13	2	4.1	3.8	58	3.3	22	35	425
13	3	4.1	3.8	34	2.1	16	13	314
13	4	4.1	3.9	22	1.4	9	16	201
14	1	7.5	5.8	60	3.8	15	14	450
14	2	7.5	5.8	50	3.0	16	10	419
14	3	7.5	5.8	41	2.3	12	9	312
15	1	4.1	5.8	60	3.2	14	11	625
15	2	4.1	5.8	41	2.1	16	20	425
15	3	4.1	5.8	28	1.4	31	15	312
15	4	4.1	5.8	19	0.9	36	13	187
16	1	7.5	5.8	80	5.4	18	6	562
16	2	7.5	5.8	68	4.3	17	15	498
16	3	7.5	5.8	53	3.3	15	17	435
17	1	4.1	5.8	100	5.8	218	119	942
17	2	4.1	5.8	67	3.4	(1)	94	653
17	3	4.1	5.8	42	2.0	(1)	26	427
17	4	4.1	5.8	26	1.2	(1)	25	251

For end landings, the torus was guided by two cables as shown in Figure A-5. Instrumentation used to measure velocity, stroke, and acceleration was similar to that used for flat landing tests. Results of end landing tests are presented in Table A-2.

TABLE A-2
MODEL DYNAMIC TEST RESULTS
END LANDING

TEST NUMBER	IMPACT NUMBER	PAYLOAD WEIGHT (LB)	INFLATION PRESSURE (LB/IN ²)	IMPACT VELOCITY (FT/SEC)	MAXIMUM PAYLOAD STROKE (IN.)	MAXIMUM LOAD FACTOR ON PAYLOAD (EARTH g'S)		
						n _z	n _y	n _x
18	1	4.4	4.2	58	8.8	21	195	21
18	2	4.4	4.2	42	7.3	9	152	9
18	3	4.4	4.2	38	4.6	5	120	7
19	1	4.4	4.2	79	11.0	28	278	62
20	1	4.4	6.0	56	8.1	24	245	14
20	2	4.4	6.0	48	6.5	20	205	9
21	1	4.4	6.0	80	10.5	36	325	25
21	2	4.4	6.0	54	7.5	(1)	208	(1)
22	1	4.4	6.0	100	13.3	40	419	38
23	1	7.8	6.0	60	8.8	16	195	8
23	2	7.8	6.0	54	8.0	17	173	6
24	1	7.8	6.0	80	11.7	32	290	14
24	2	7.8	6.0	72	10.1	22	245	9